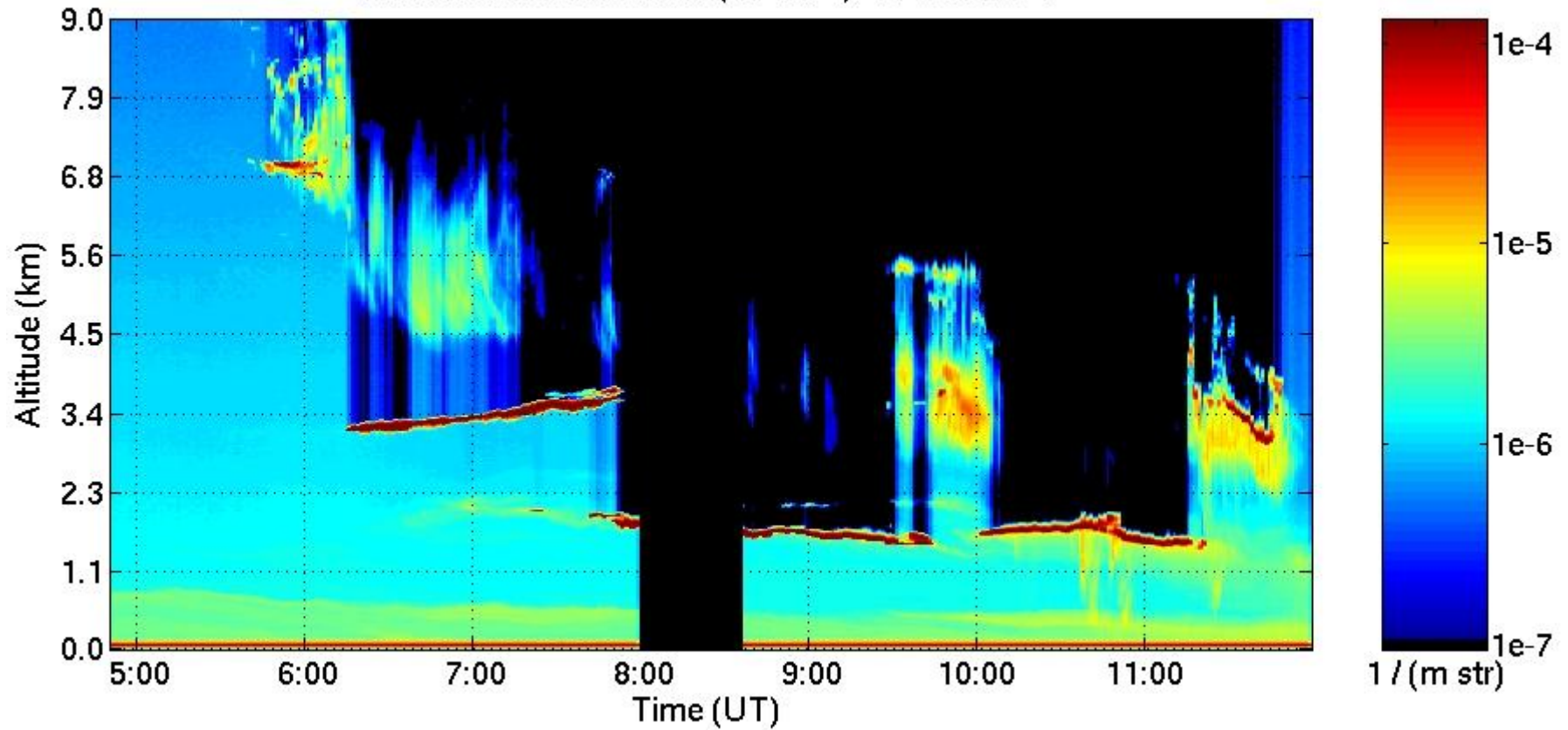


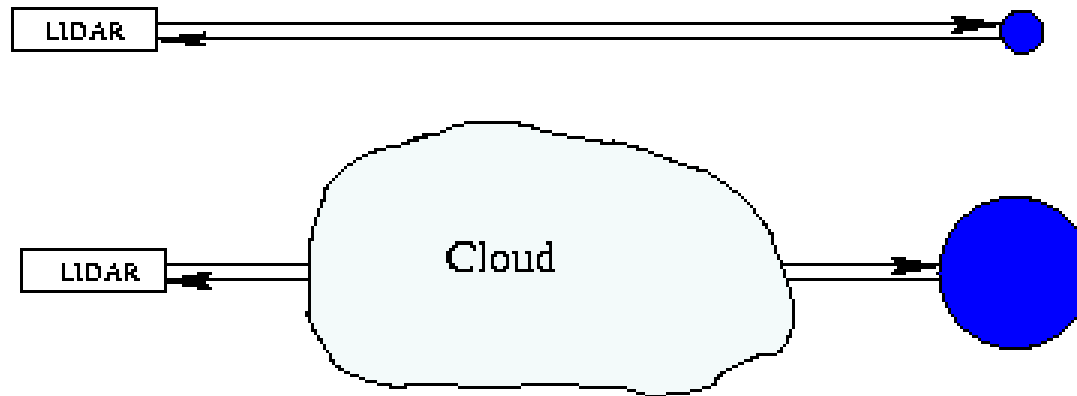
HSRL data processing from TORERO
Ed Eloranta



Attenuated backscatter ($\text{m}^{-1} \text{str}^{-1}$) 14-Jan-2004



$$P(r) \sim \beta_s(r) \frac{\mathcal{P}(180, r)}{4\pi} \exp(-2 \int_0^r \beta_e(r) dr)$$



Traditional aerosol lidar can not distinguish between changes in target reflectivity and attenuation between the lidar and the target

$$\rho_a(r) \propto \frac{1}{r^2} \cdot \frac{P(180,r)}{4\pi} \beta_a(r) \cdot \exp(-2 \int (\beta_a(r) + \beta_m(r)) \cdot dr) - \text{aerosol return,}$$

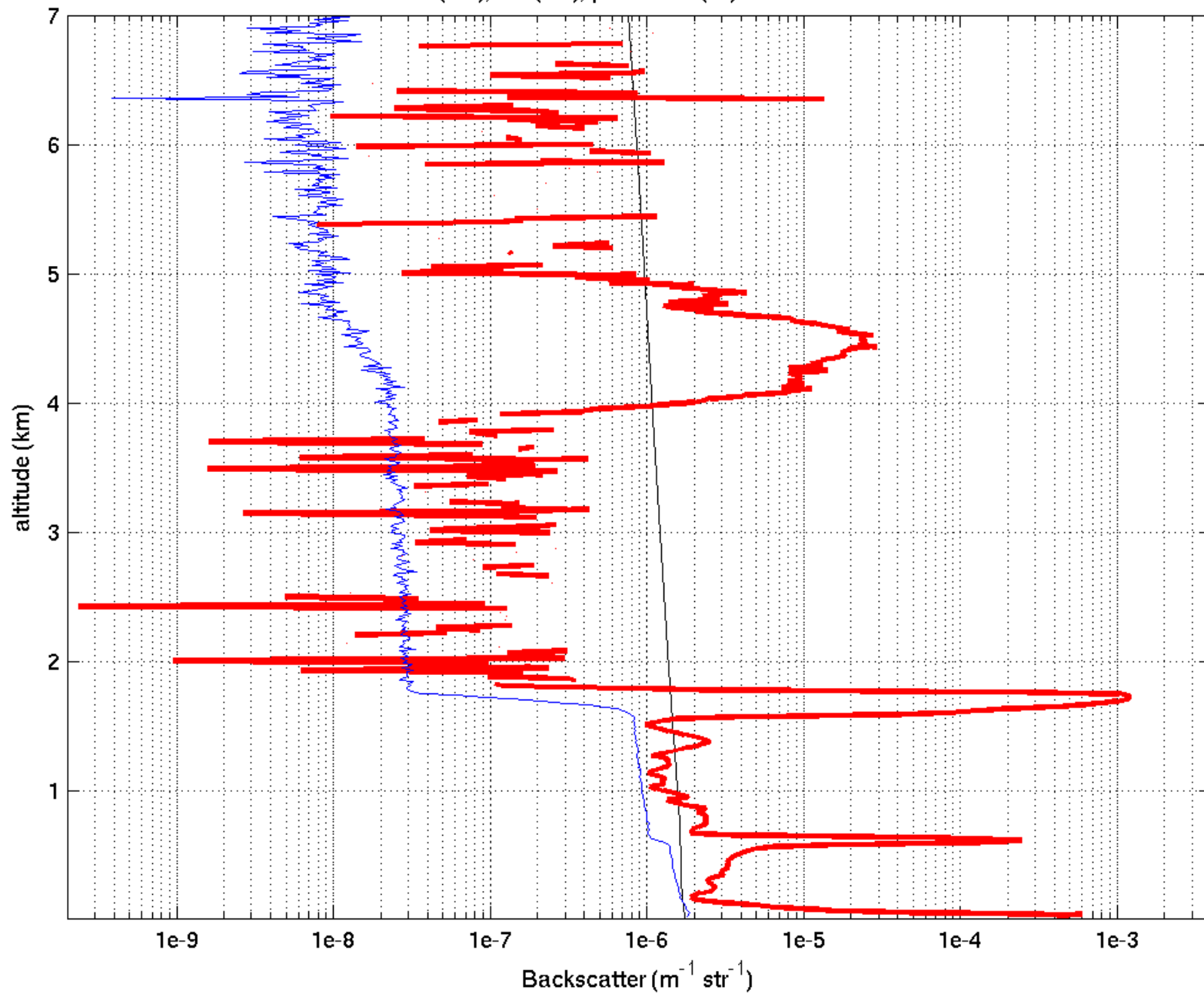
$$\rho_m(r) \propto \frac{1}{r^2} \cdot \frac{3}{8\pi} \beta_m(r) \cdot \exp(-2 \int (\beta_a(r) + \beta_m(r)) \cdot dr) - \text{molecular return}$$

$$\beta'_a(r) = \frac{P(180,r)}{4\pi} \cdot \beta_a(r) = \frac{3}{8\pi} \cdot \beta_m(r) \cdot \frac{\rho_a(r)}{\rho_m(r)}$$

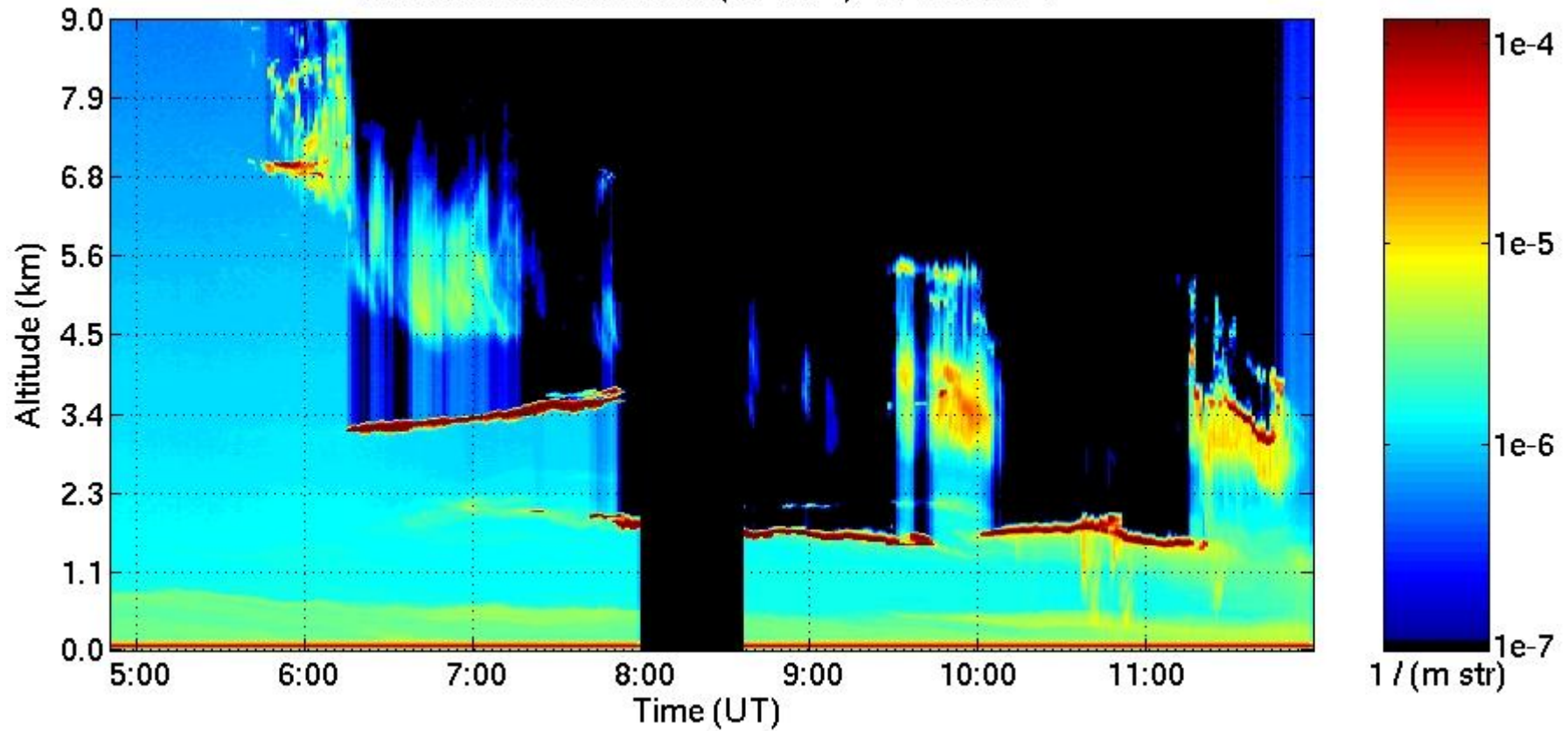
The optical depth between r_1 and r_2 is derived by comparing the molecular return to that expected from a purely molecular atmosphere:

$$\tau(r_1, r_2) = \frac{1}{2} \cdot \log\left(\frac{r_1^2 \rho(r_2) \cdot \rho_m(r_1)}{r_2^2 \rho(r_1) \cdot \rho_m(r_2)}\right)$$

attenuated mol(blu), mol(blk), particulate(rd) 05-Nov-04 19:59->20:02

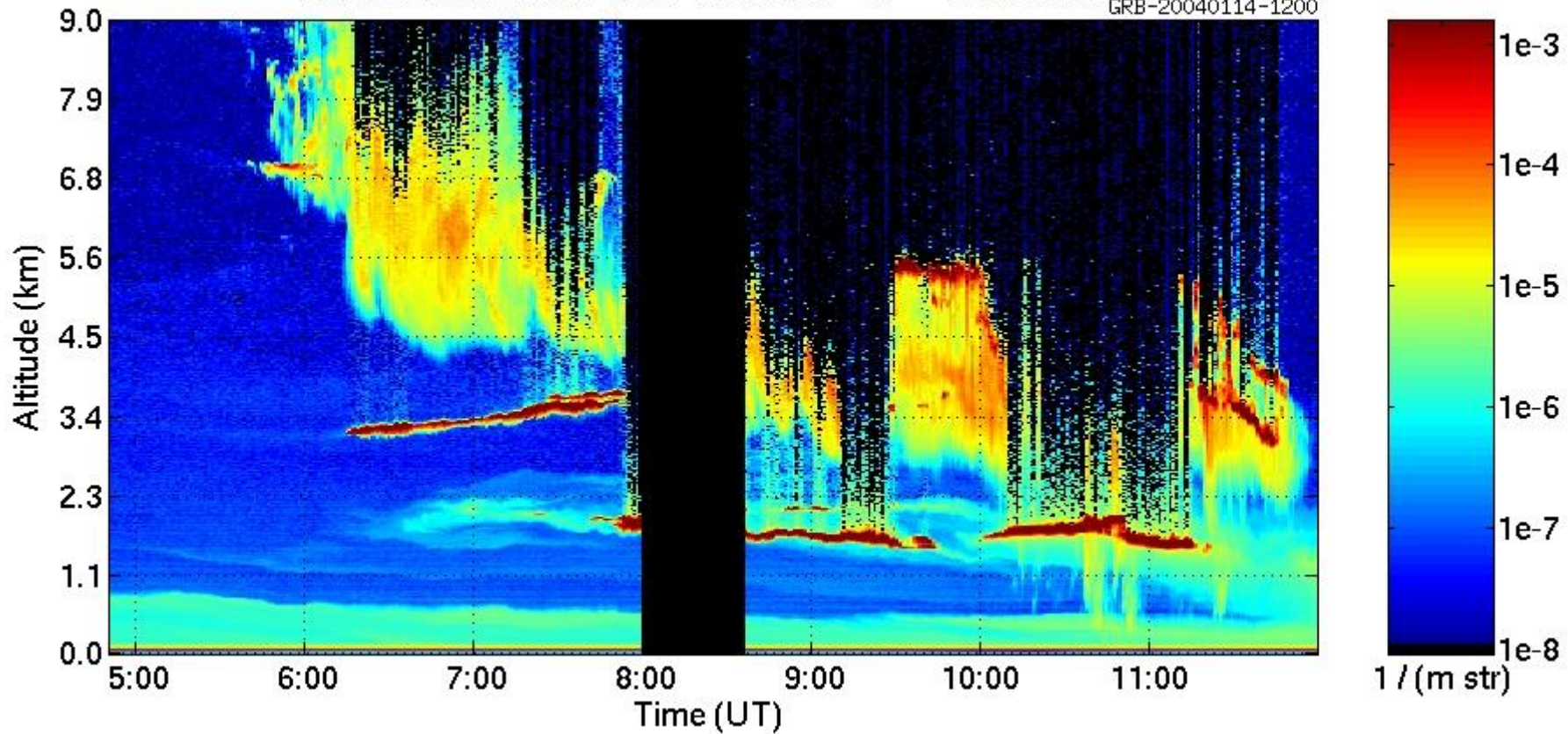


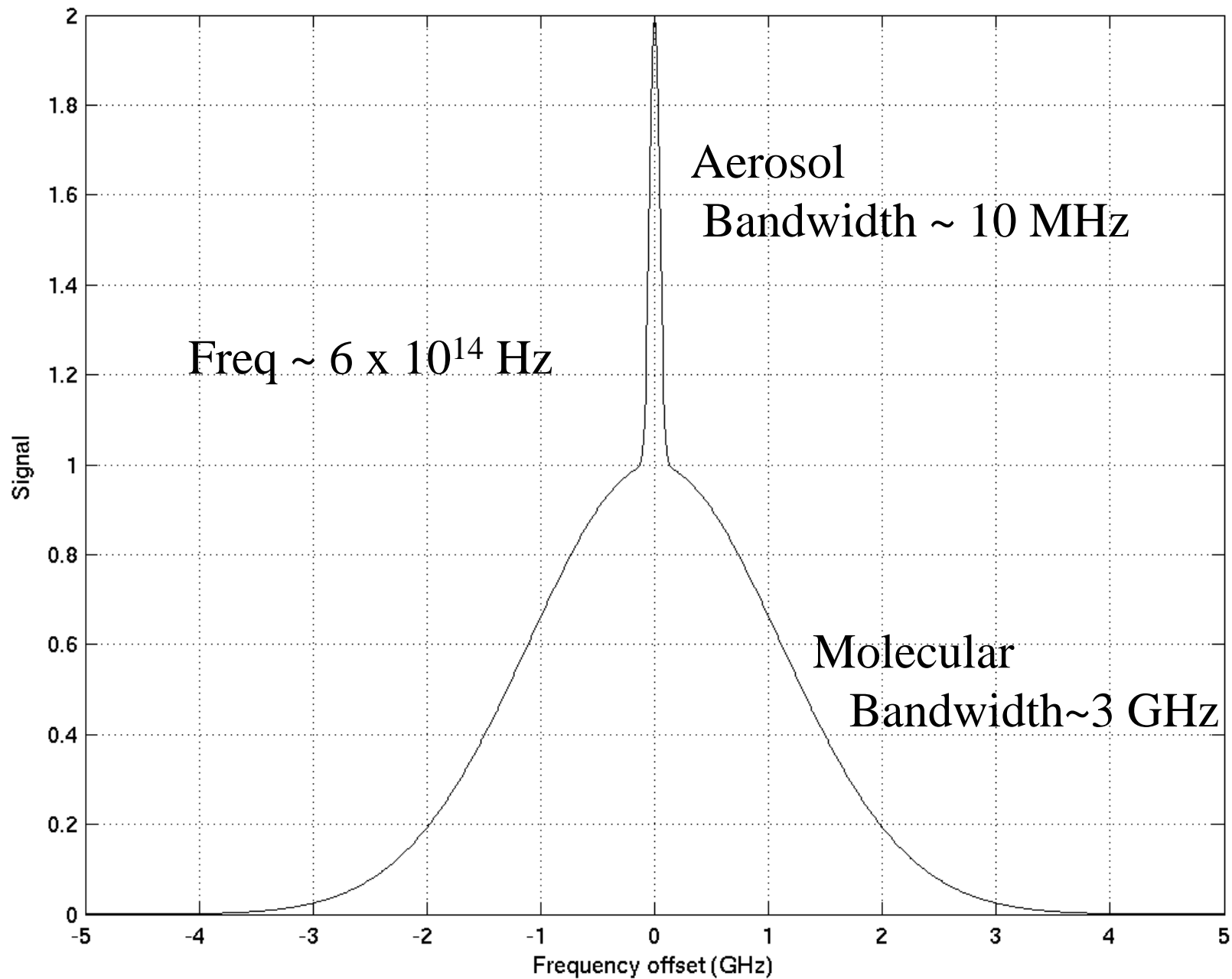
Attenuated backscatter ($\text{m}^{-1} \text{str}^{-1}$) 14-Jan-2004



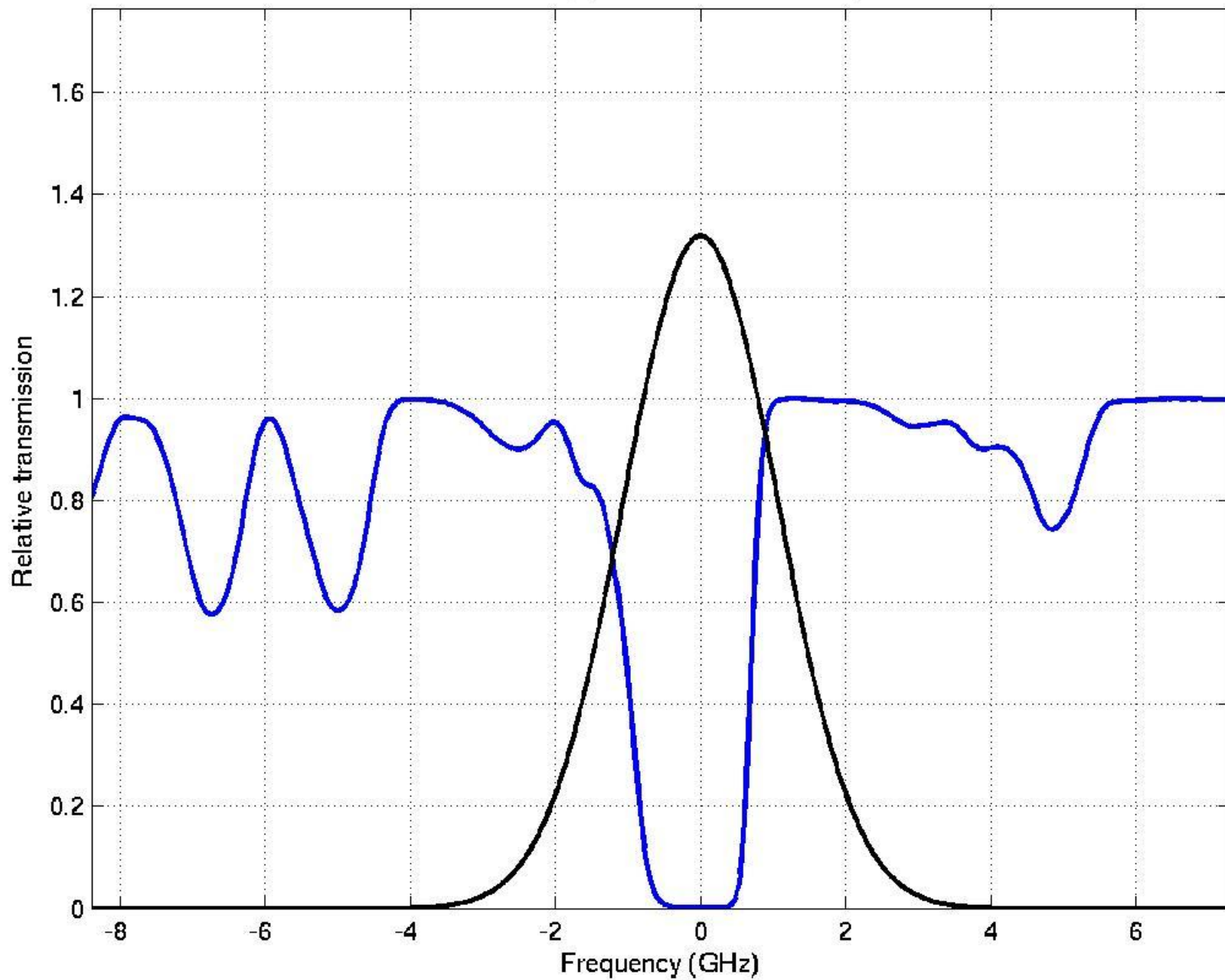
Aerosol backscatter cross section $\text{m}^{-1} \text{str}^{-1}$ 14-Jan-2004

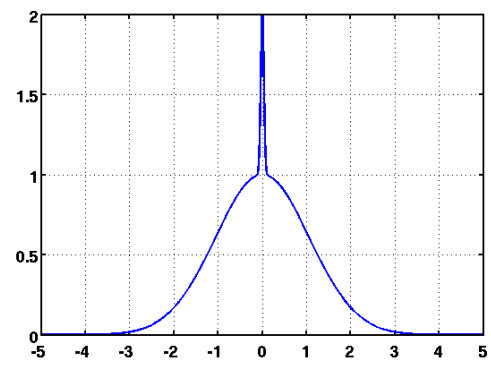
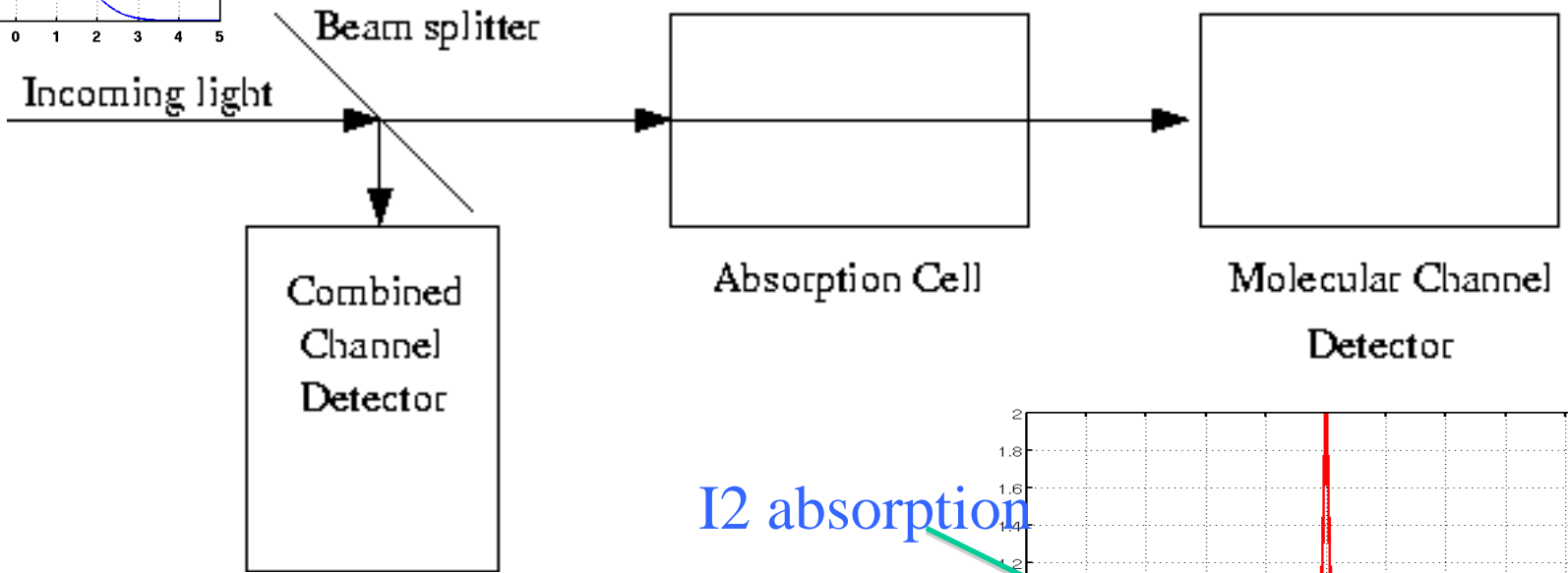
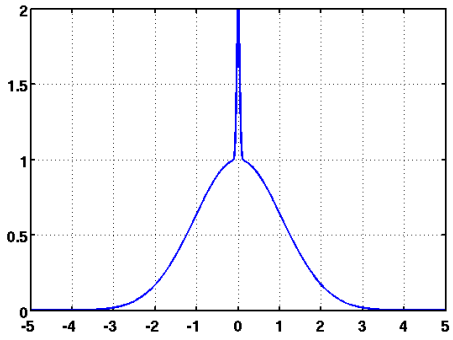
GRB-20040114-1200



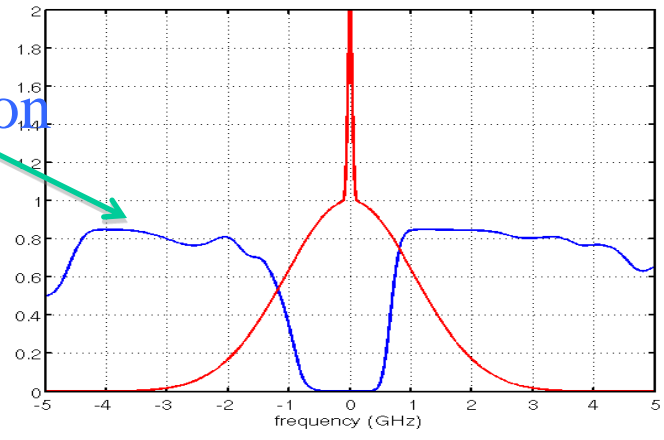


12 cell transmission and Doppler broadened Atmospheric Backscatter



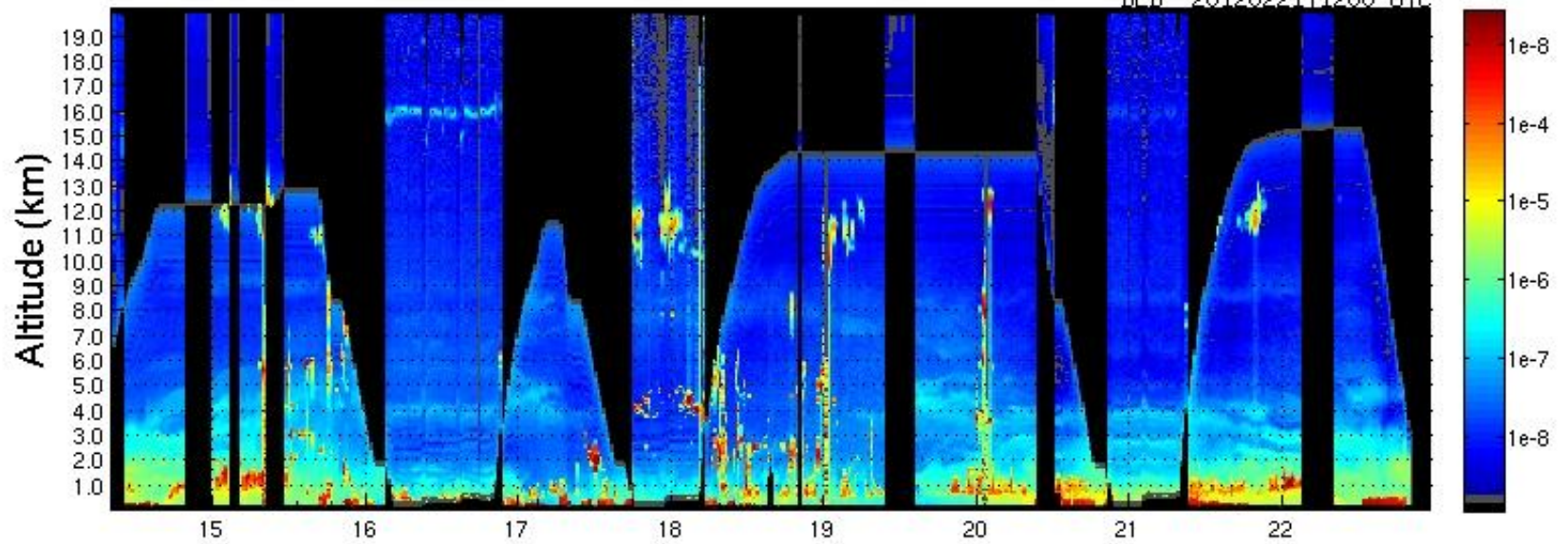


I₂ absorption

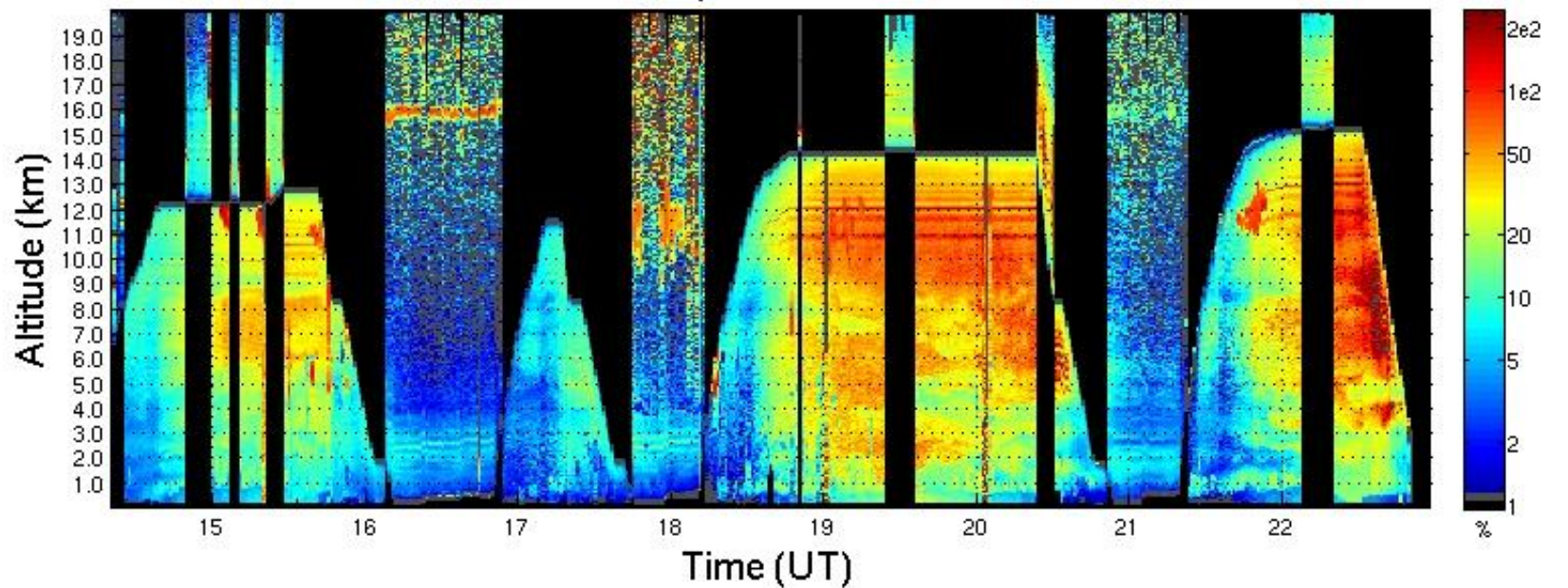


Aerosol backscatter cross section 22-Feb-2012

BLR 20120221T1200 UTC

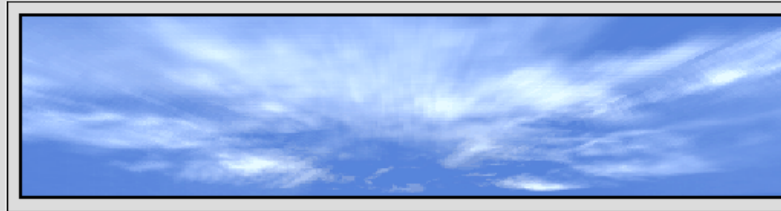


Particulate circular depolarization ratio 22-Feb-2012



<http://lidar.ssec.wisc.edu>

Welcome to the University of Wisconsin Lidar Group



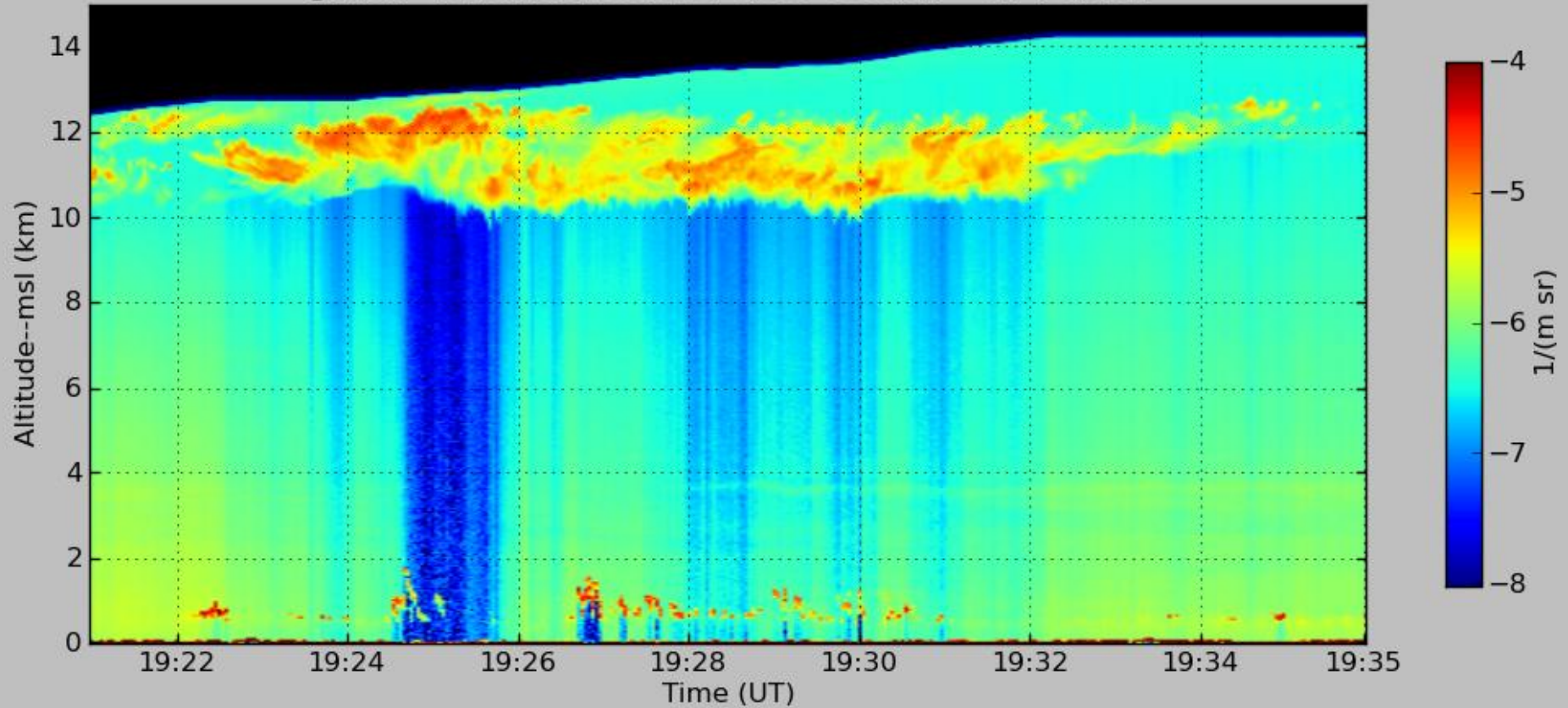
- [About this image...](#)

Index of Topics

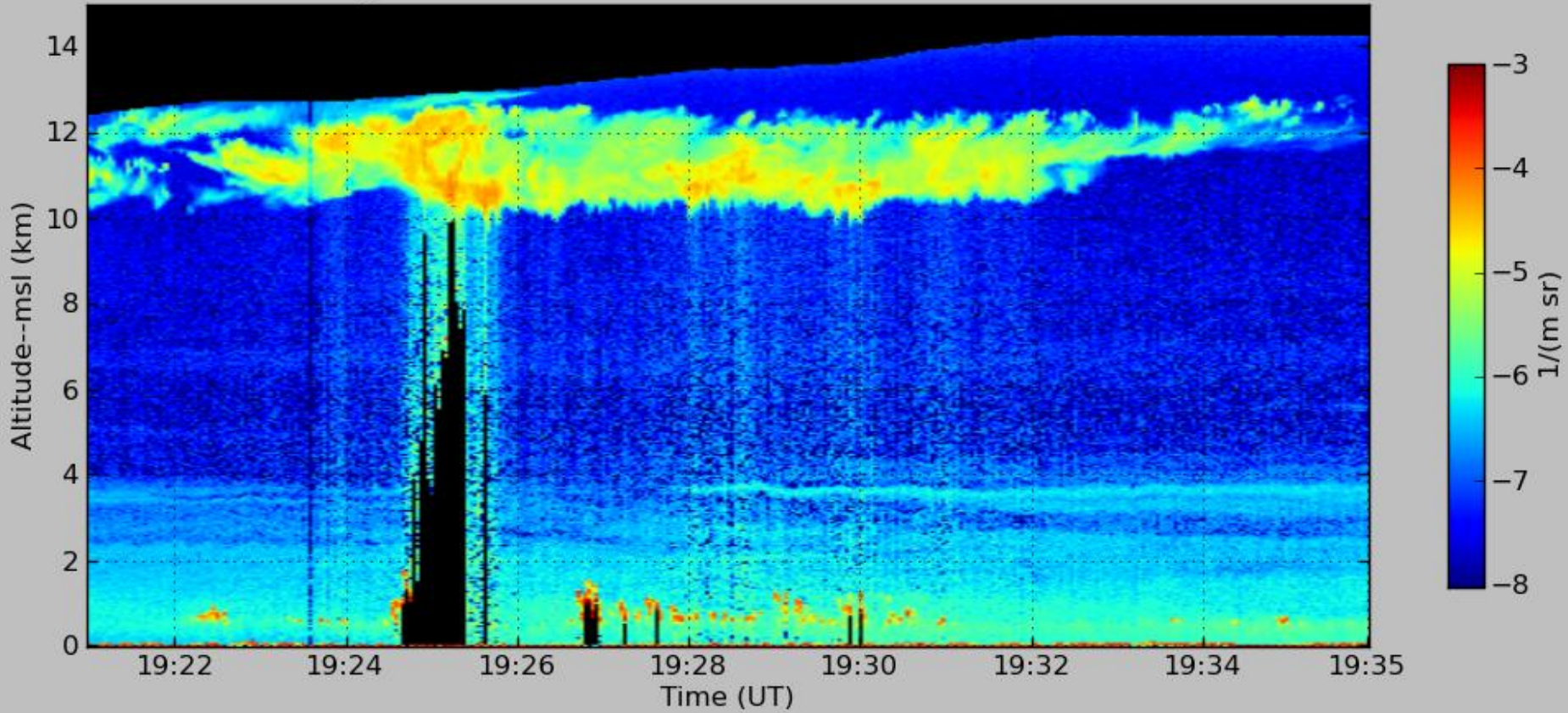
- [Arctic HSRL](#): A new lidar designed for long term observations in the Arctic
- [Data: HSRL, MMCR, PAERI, MWR](#) Web access to data acquired after 01-May-2004
- [Volume Imaging Lidar](#): System description
- [High Spectral Resolution Lidar](#): System description(van mounted system used prior to May 2004)
- [Lidar Images](#): Thousand's of Lidar images acquired before 2004
- [Movies](#): MPEG animations generated from VIL data
- [HSRL with MODIS](#): Data at Satellite Overpasses, for MODIS Instrument
- [Vis5D Images](#): 3-D scattering volumes produced from VIL data
- [Project Results](#): Data products and science results from selected projects
- [Publications](#): List of Lidar Group publications
- [Operation Times and Statistics](#): Some HSRL and VIL experiments prior to 1998
- [Staff](#): UW Lidar Group staff and contact information
- [Results from Lake-ICE](#): Lake-Induced Convection Experiment



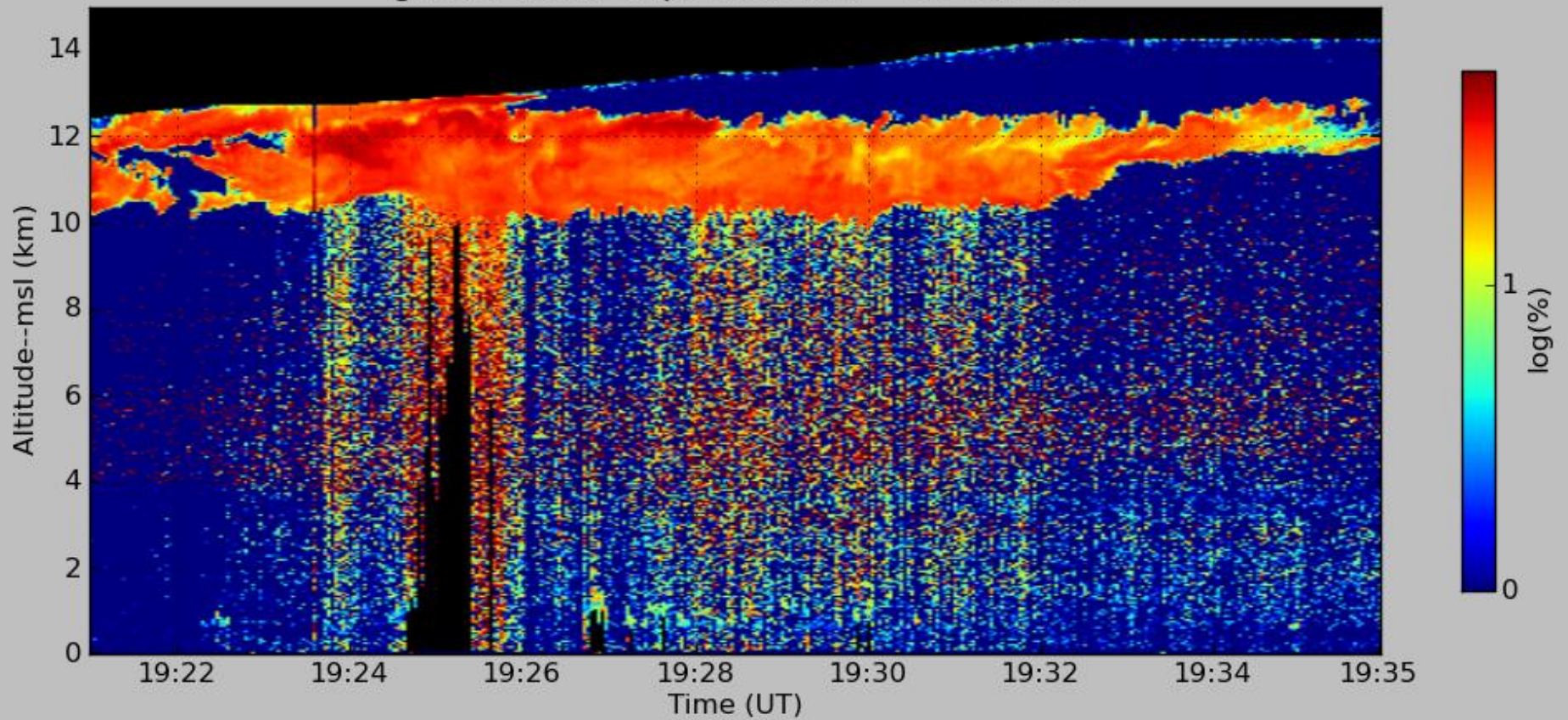
gvhsrl atten backscatter cross section 24-Feb-12



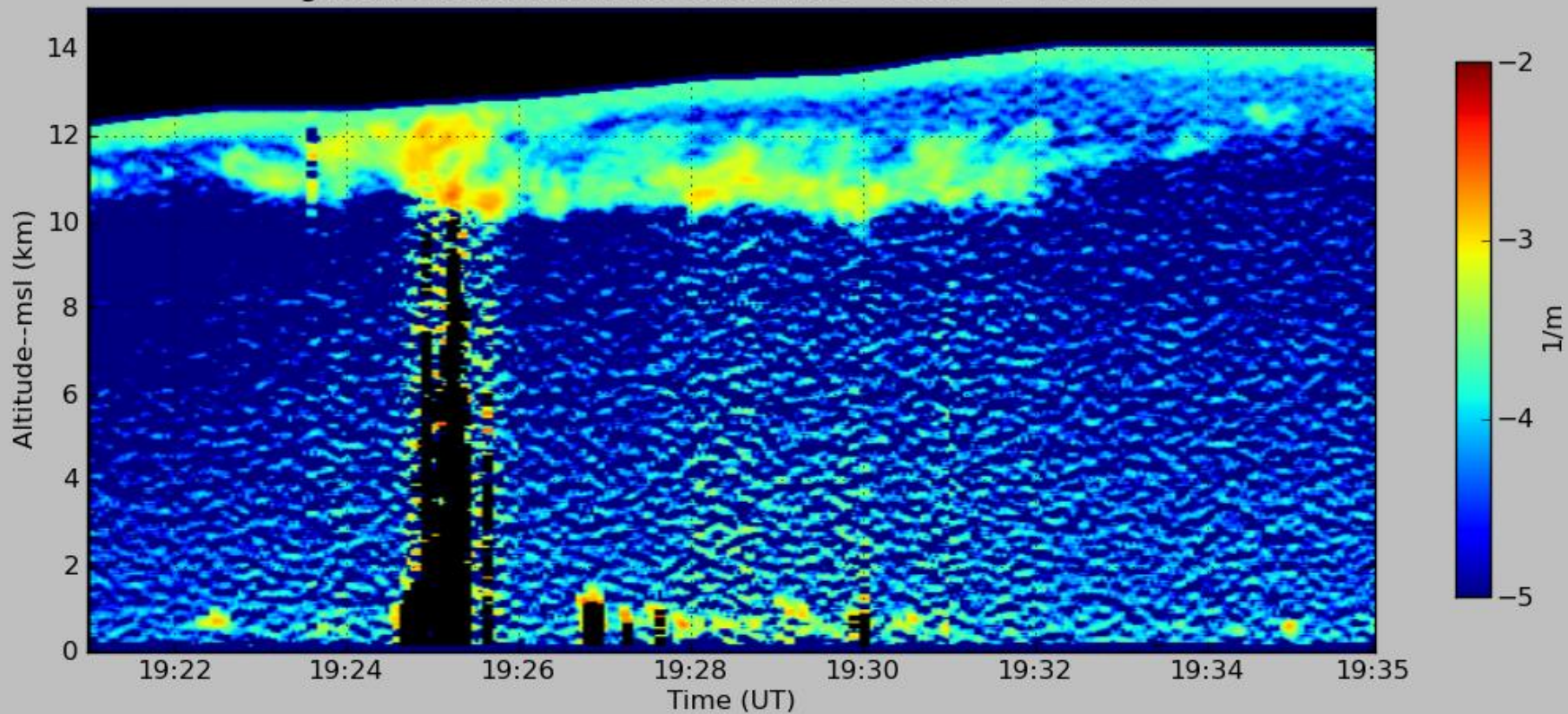
gvhsrl backscatter cross section 24-Feb-12



gvhsrl linear depolarization 24-Feb-12



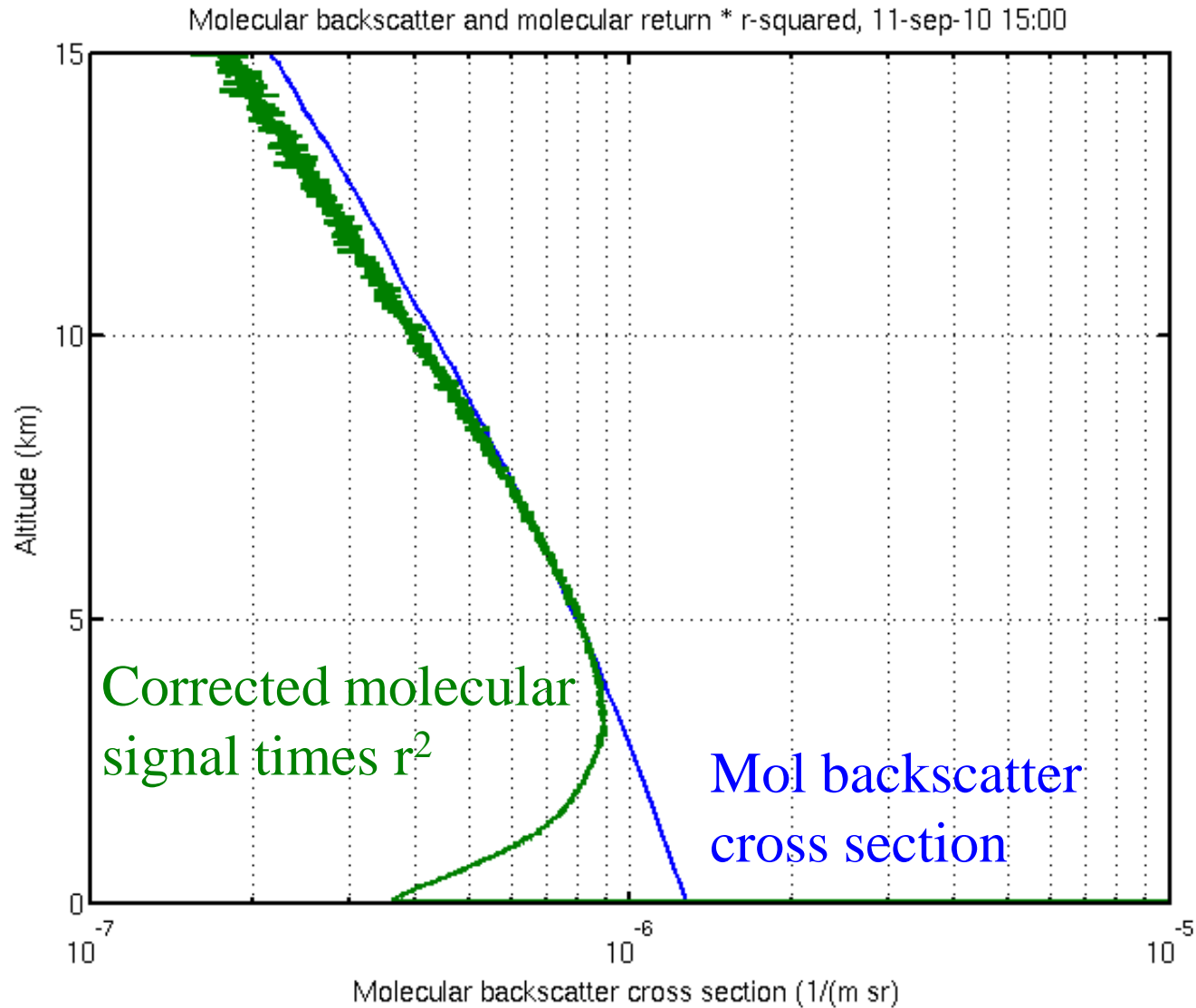
gvhsrl extinction cross section, dz= 180.0 24-Feb-12



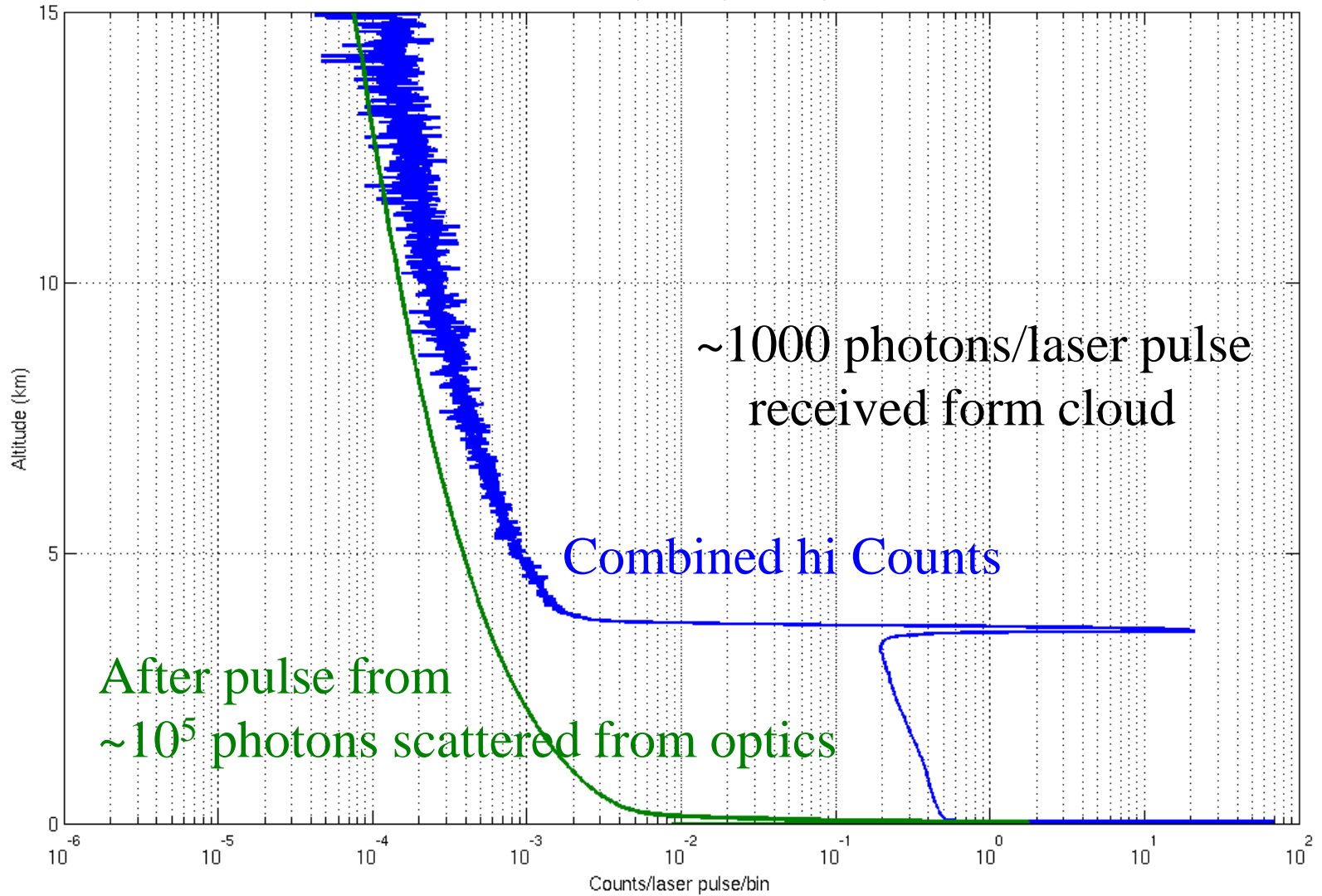
HSRL data processing corrections

- 1) Pileup correction
- 2) Baseline correction
- 3) Differential geometry correction
- 4) Geometry correction
- 5) Conversion from range to altitude
- 6) Signal time and range averaging
- 7) Molecular particulate signal separation
- 8) Compute extinction from derivative of molecular return

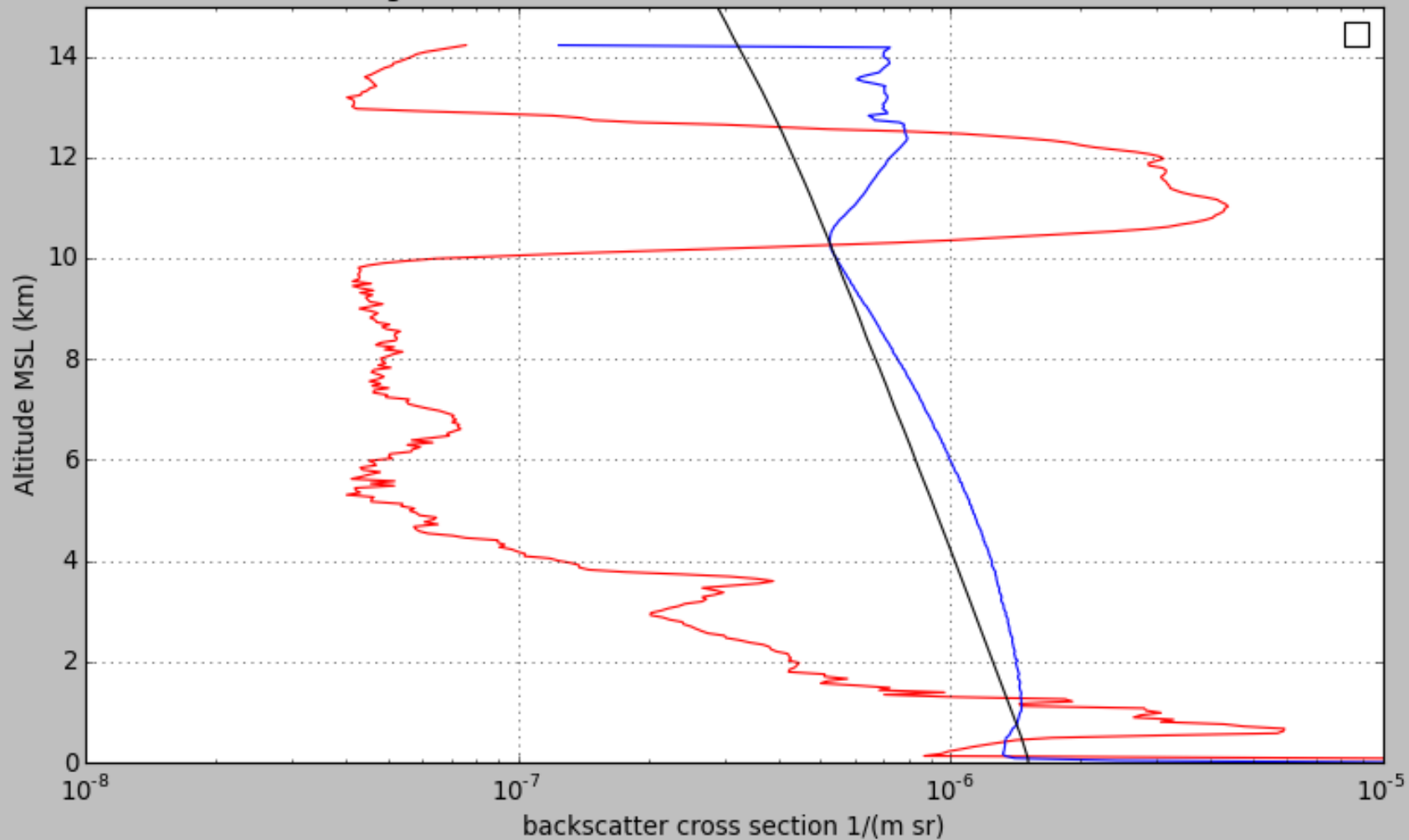
As the laser pulse propagates away from system the image size on the detector changes



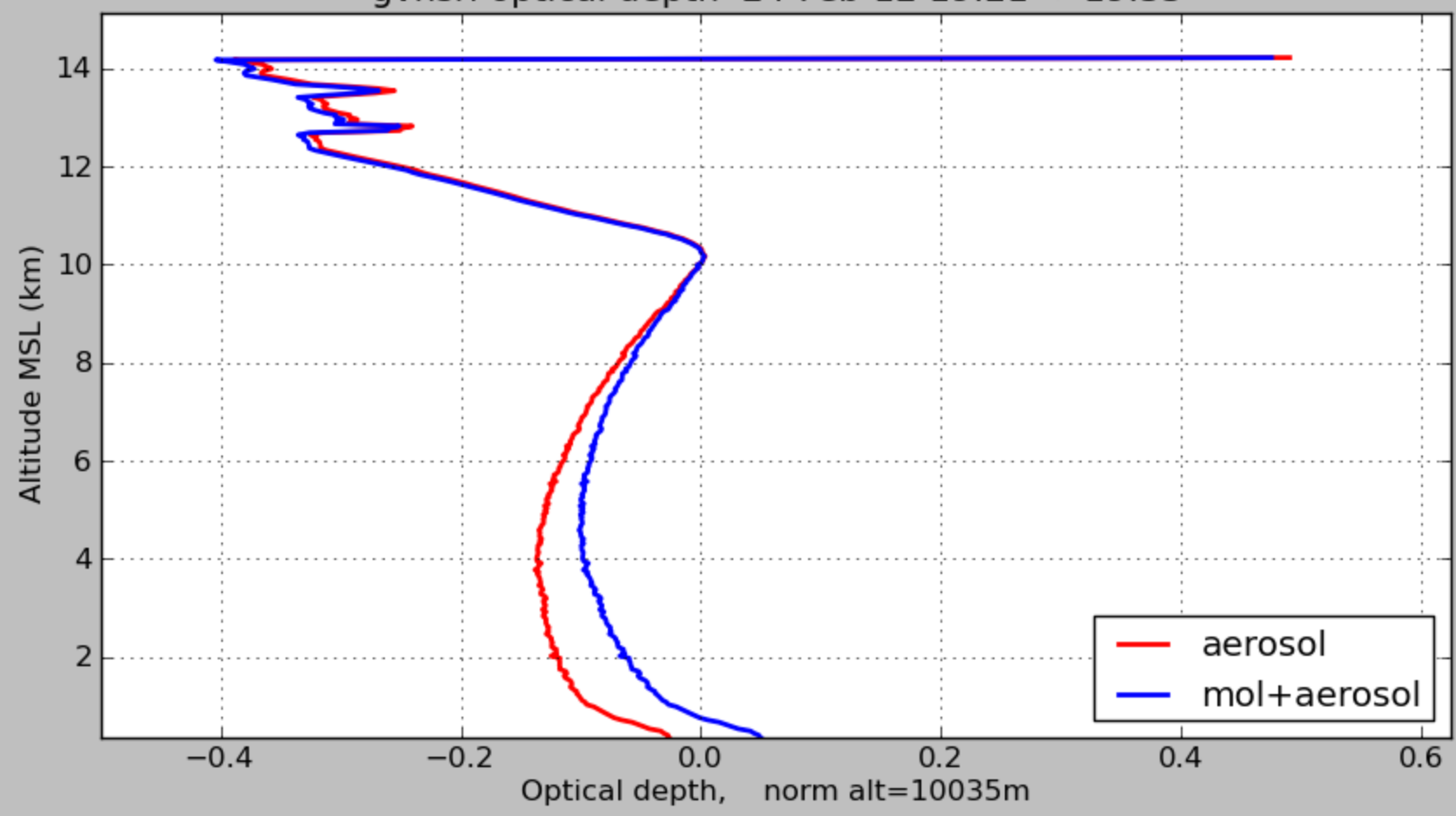
Aerosol return and laser pulse afterpulse 11-sep-10 3:30 UT



gvhsrl backscatter 24-Feb-12 19:21-->19:35

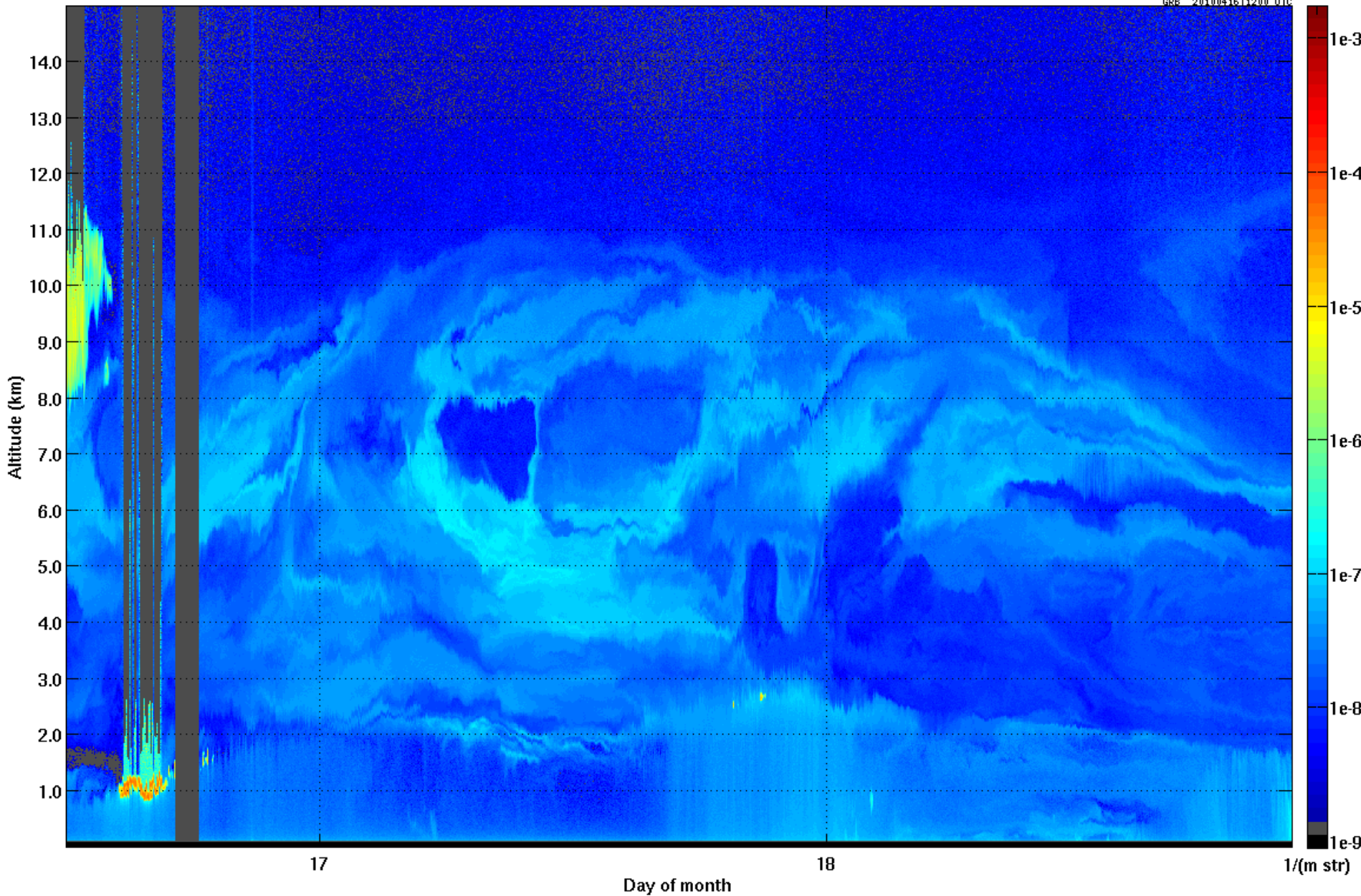


gvhsrl optical depth 24-Feb-12 19:21-->19:35

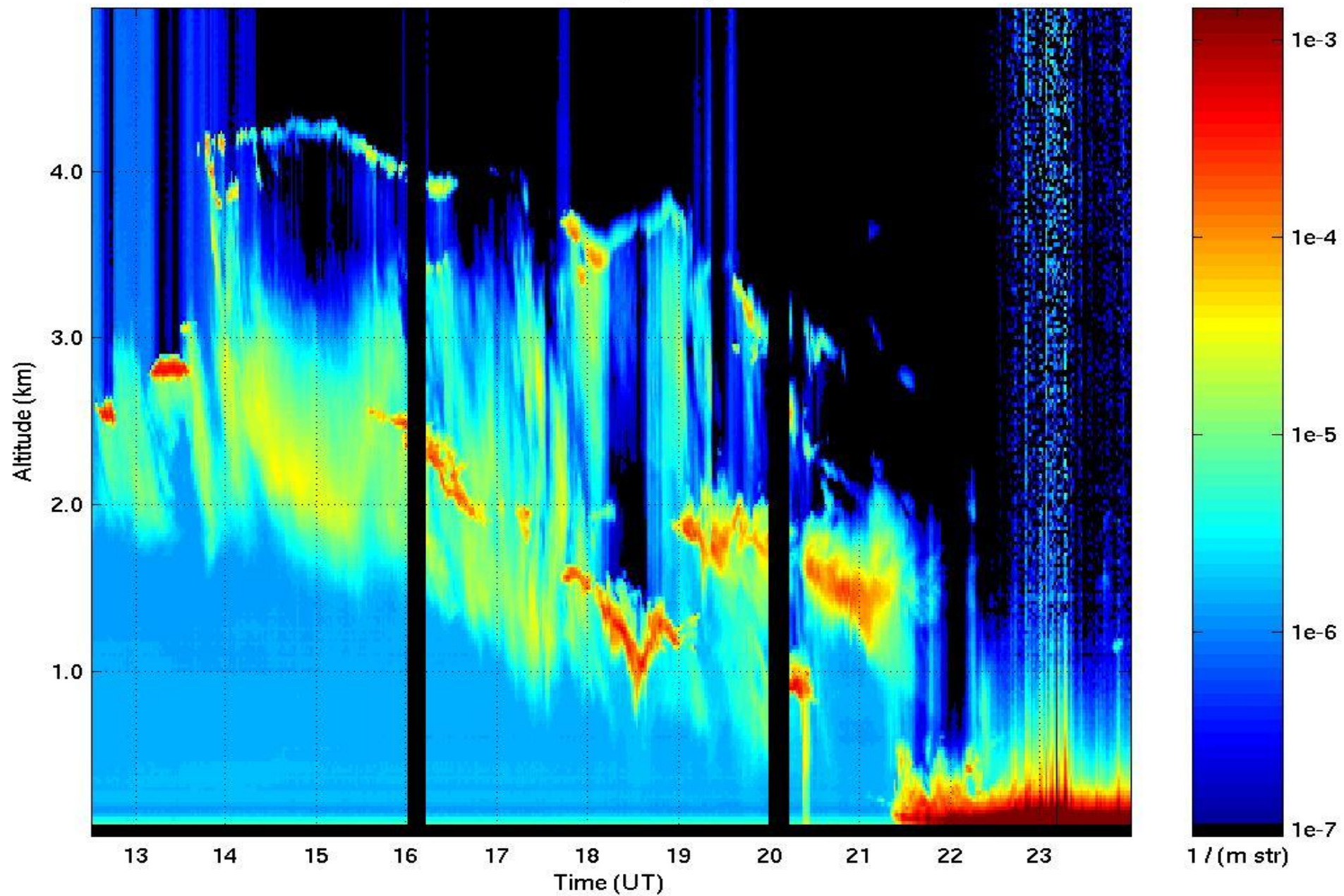


Aerosol backscatter cross section 16-Apr-2010

GRB_20100416T1200 UTC

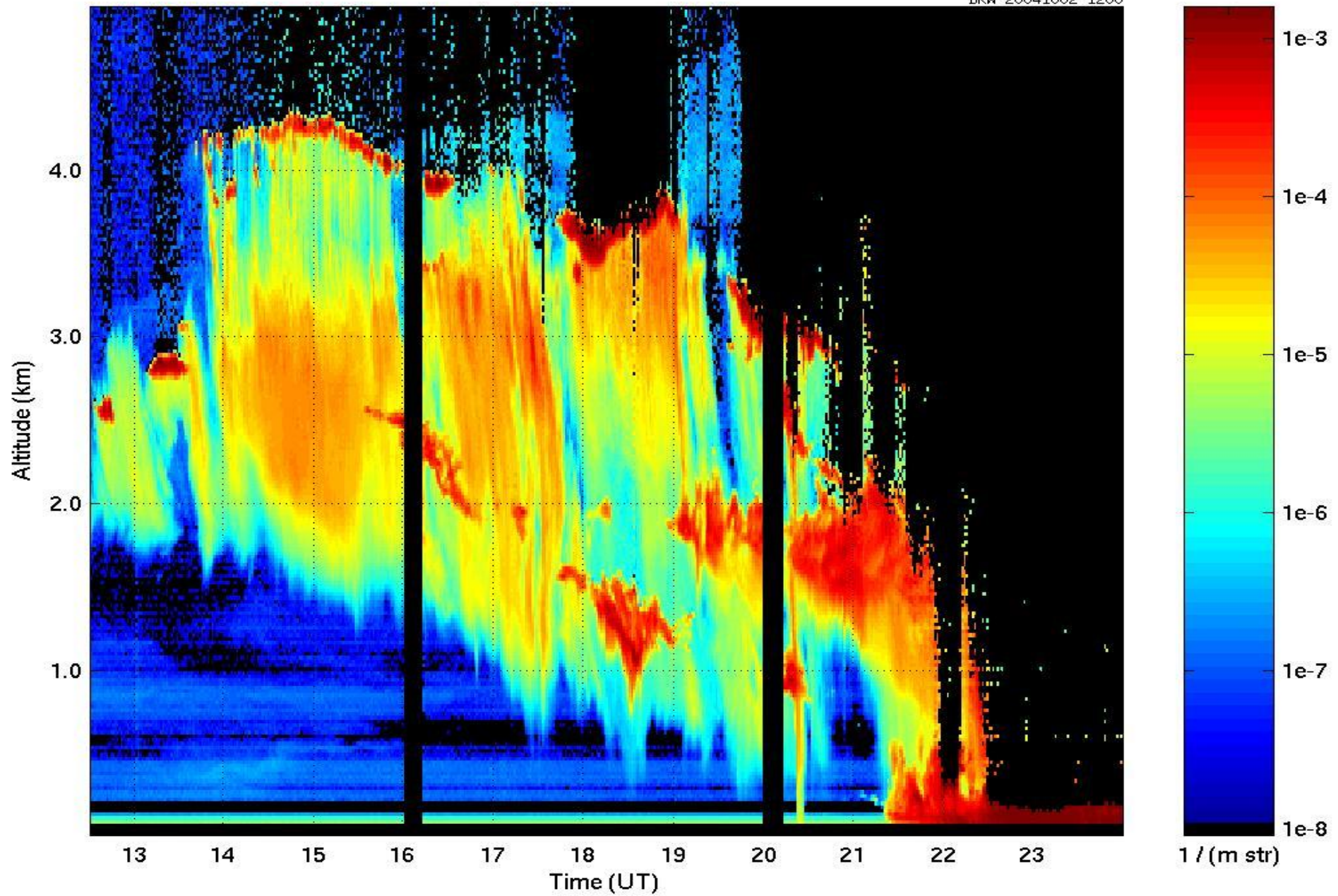


Attenuated backscatter ($\text{m}^{-1}\text{str}^{-1}$) 02-Oct-2004



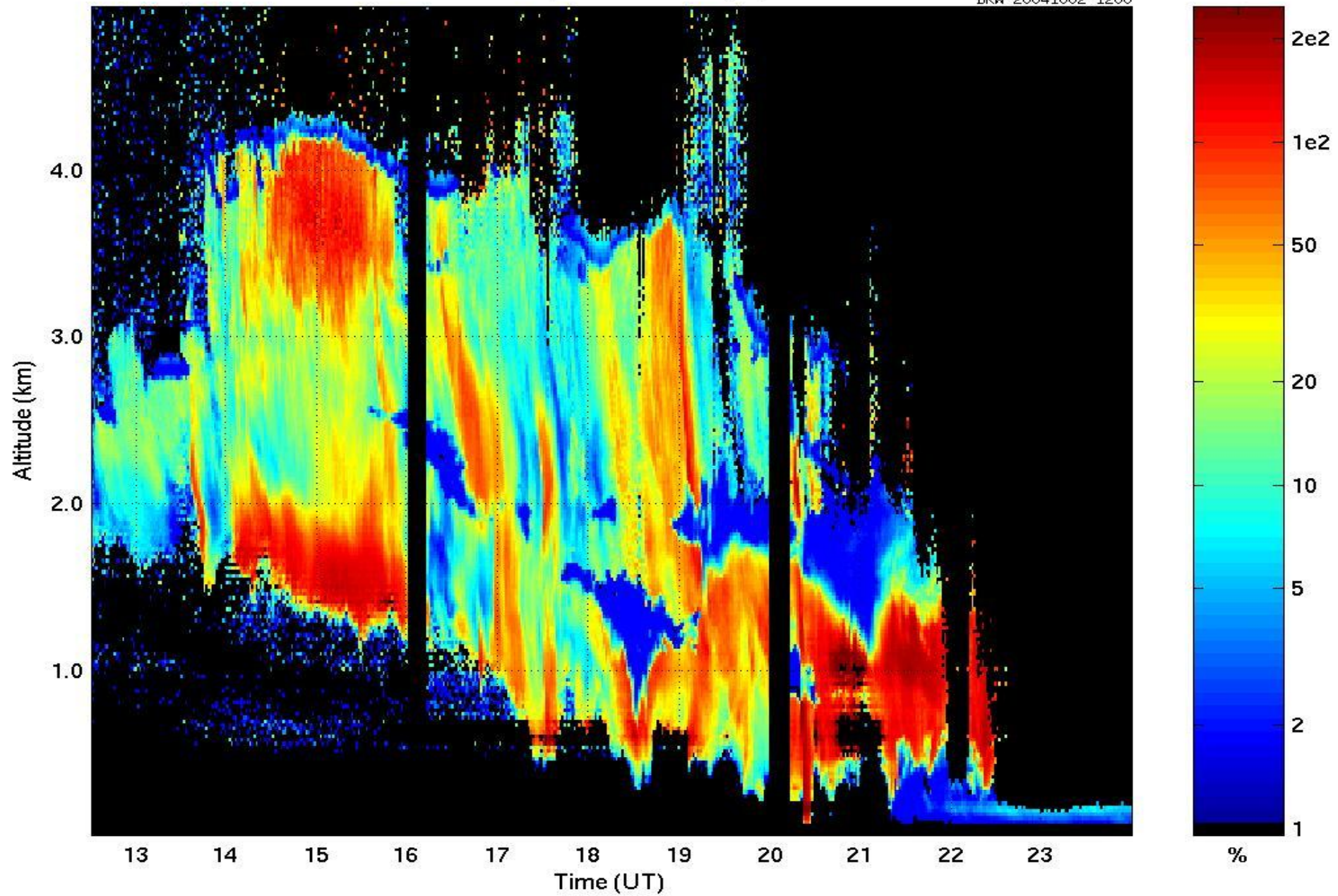
Aerosol backscatter cross section $\text{m}^{-1}\text{str}^{-1}$ 02-Oct-2004

BRW-20041002-1200

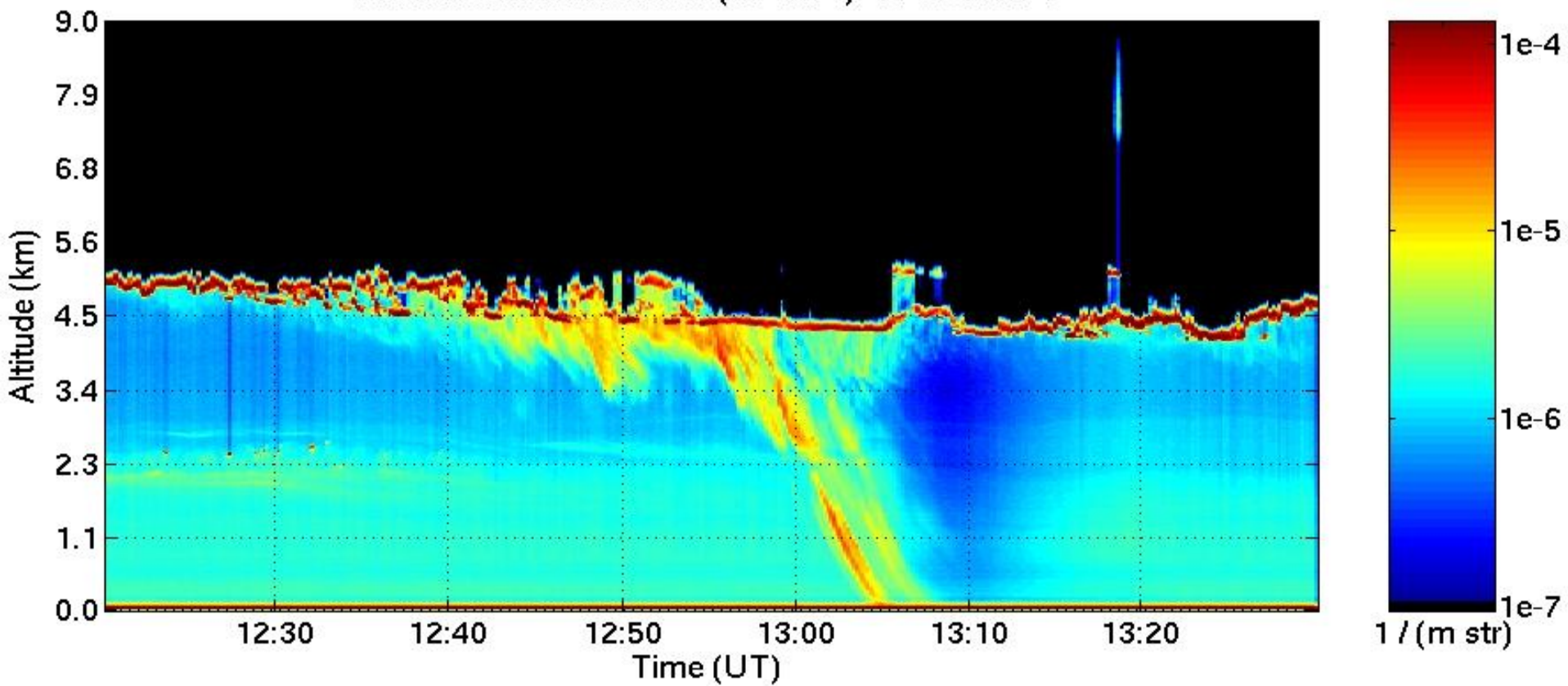


Particulate circular depolarization ratio(%) 02-Oct-2004

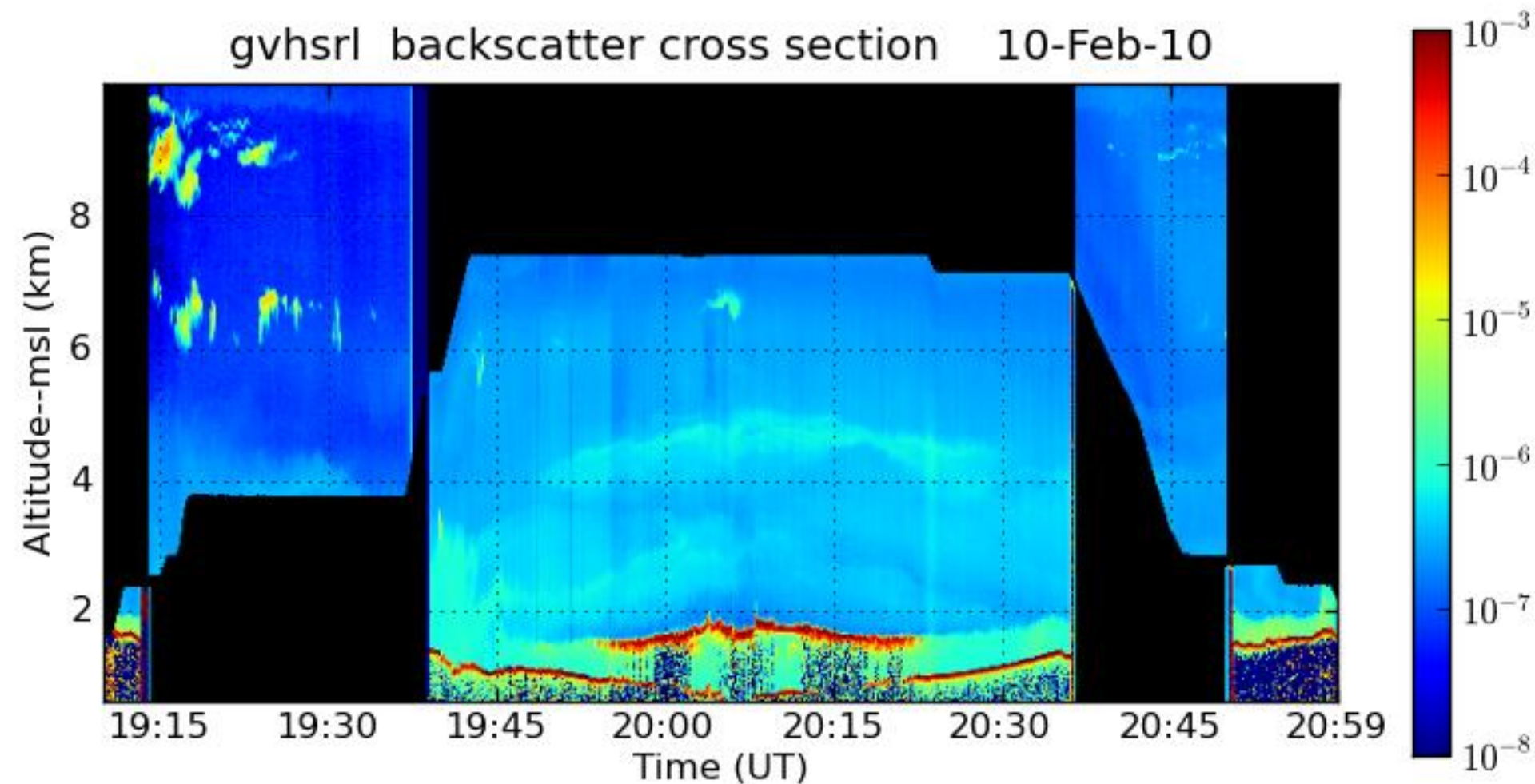
BRW-20041002-1200



Attenuated backscatter ($\text{m}^{-1} \text{str}^{-1}$) 14-Jun-2004

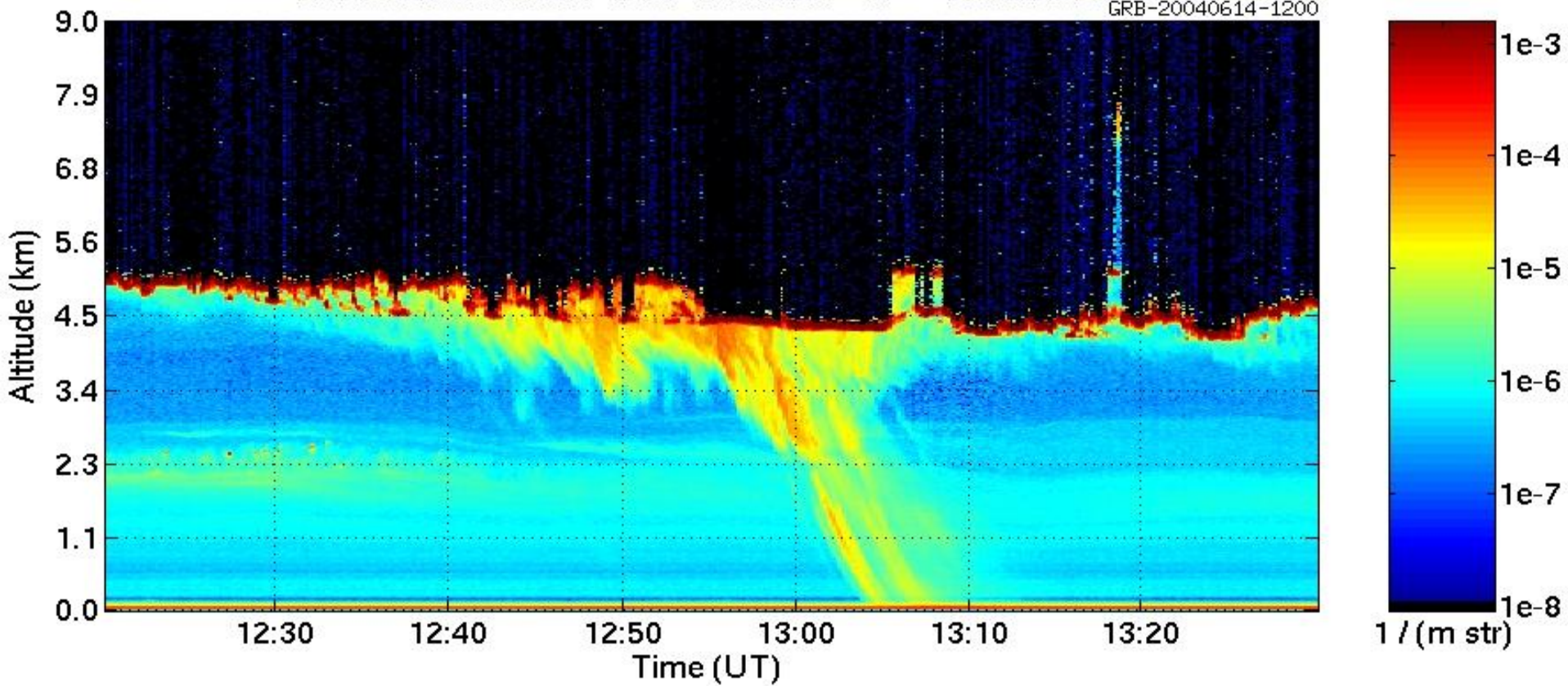


gvhsrl backscatter cross section 10-Feb-10

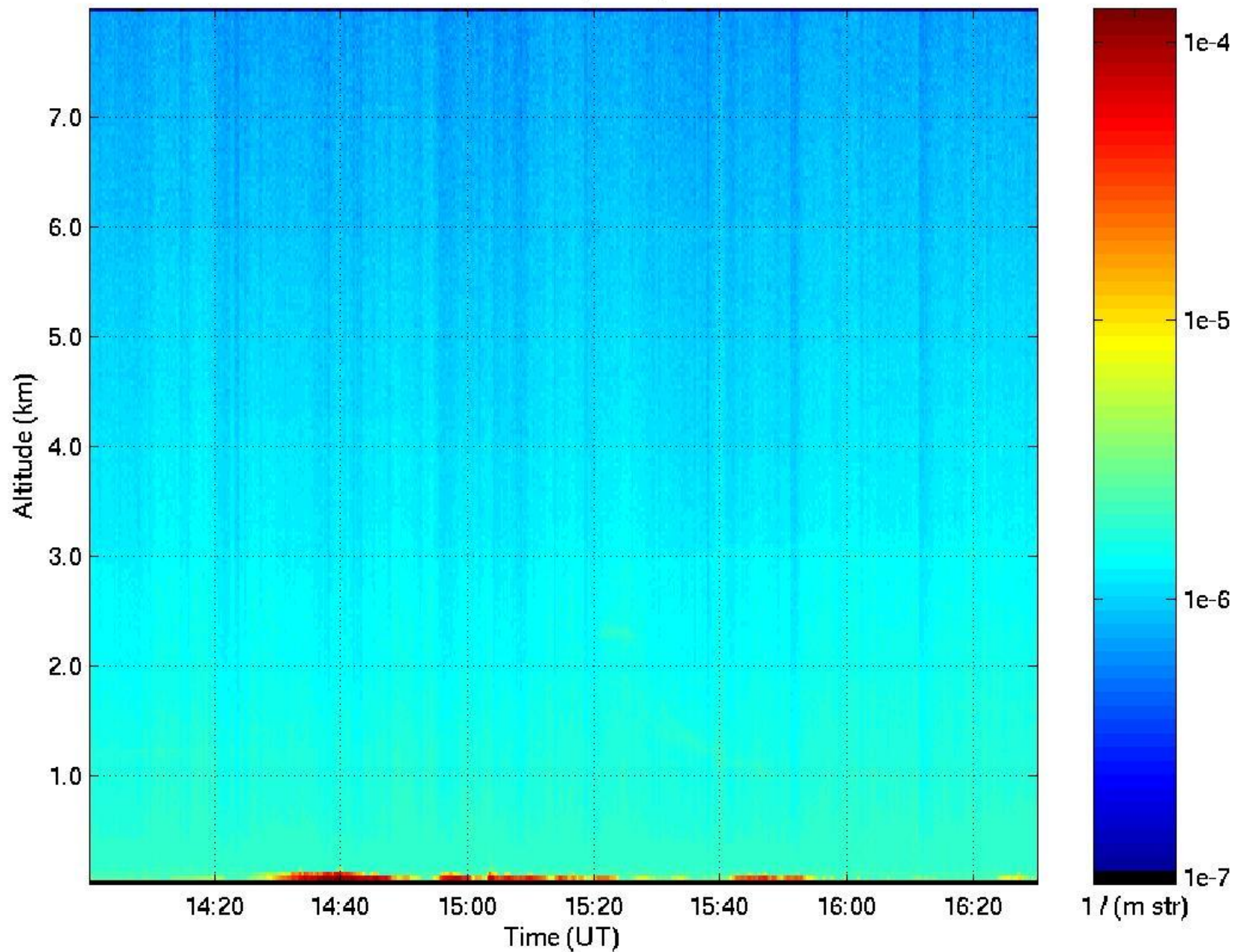


Aerosol backscatter cross section $\text{m}^{-1} \text{str}^{-1}$ 14-Jun-2004

GRB-20040614-1200

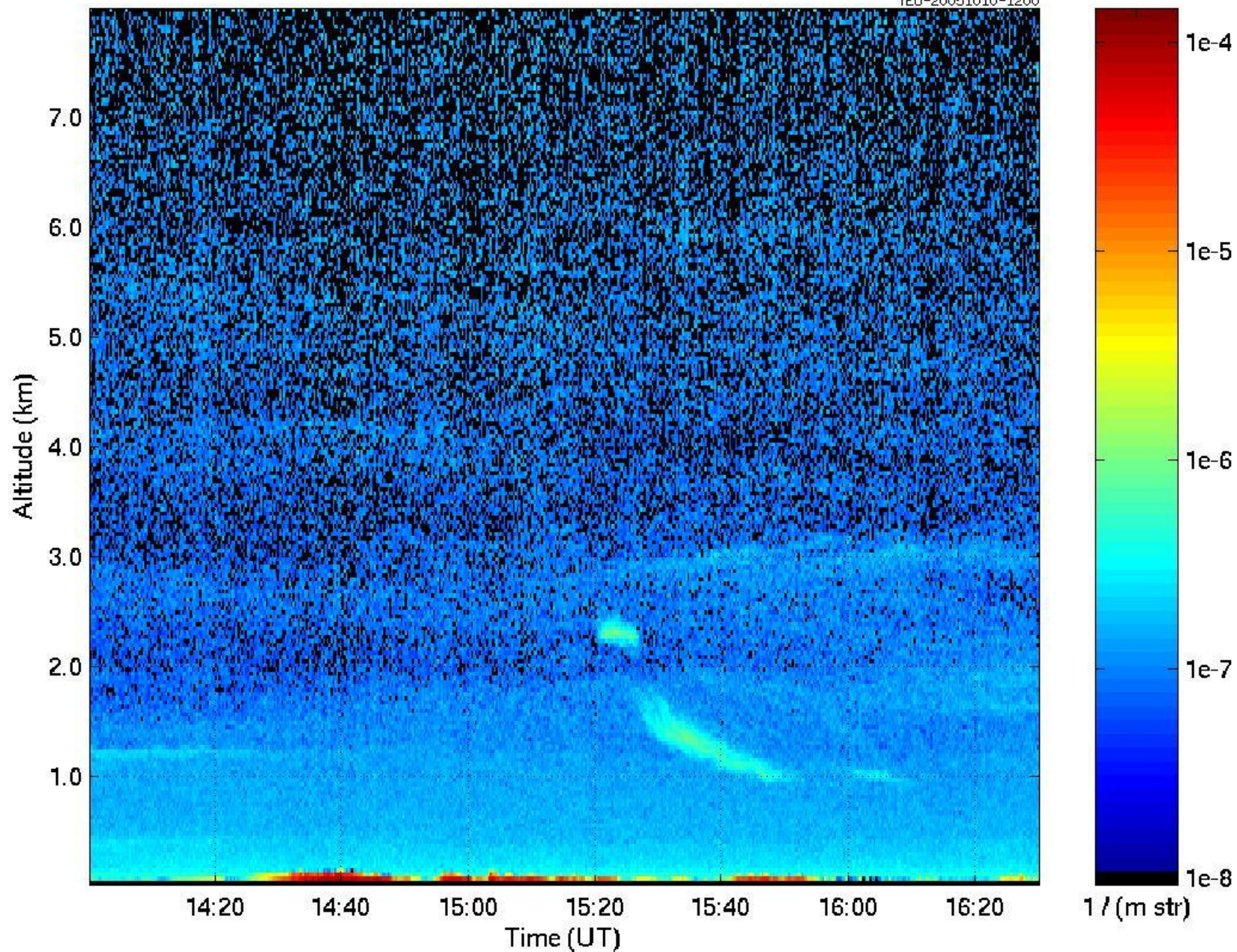


Attenuated backscatter ($\text{m}^{-1}\text{str}^{-1}$) 10-Oct-2005



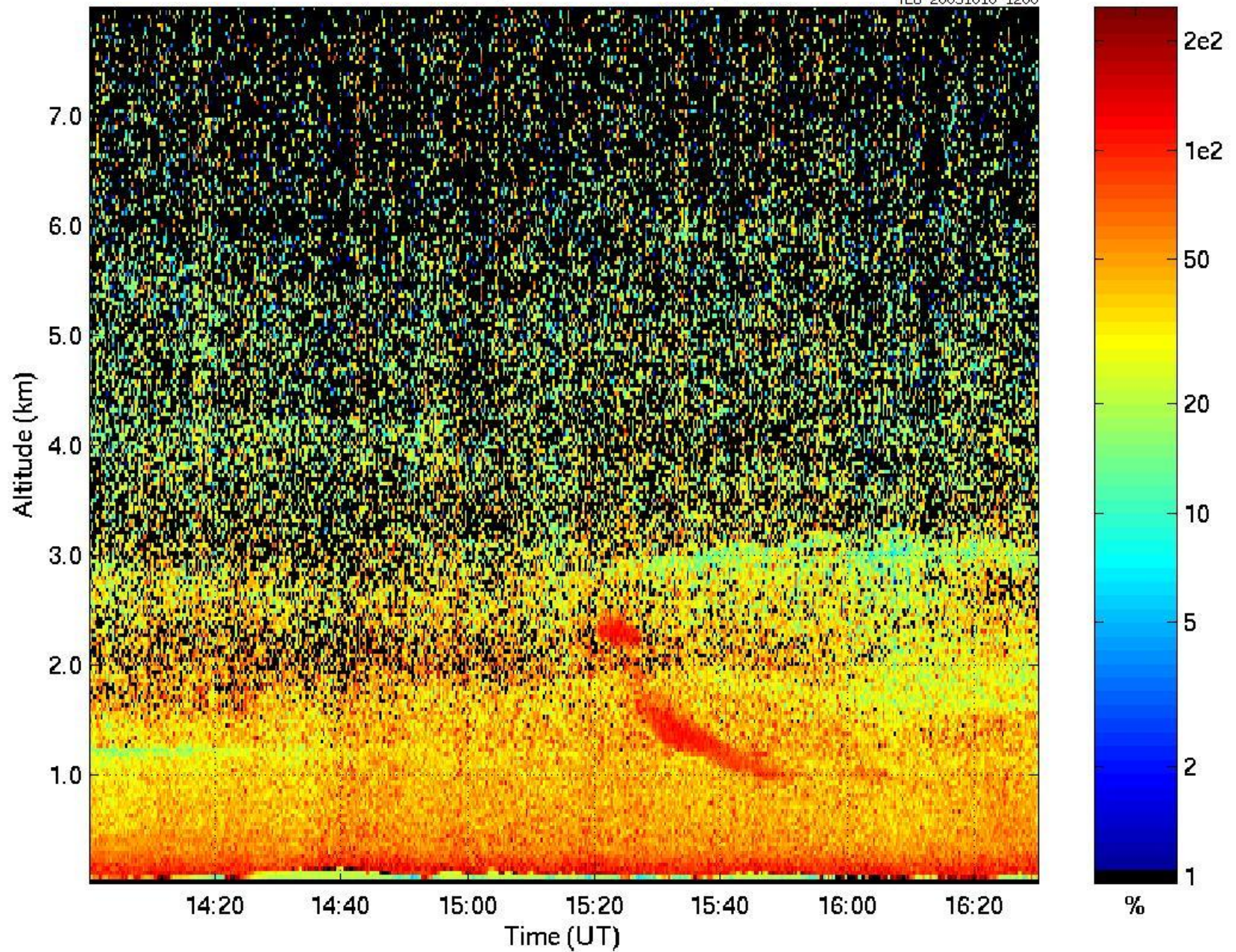
Aerosol backscatter cross section $\text{m}^{-1}\text{str}^{-1}$ 10-Oct-2005

YEU-20051010-1200



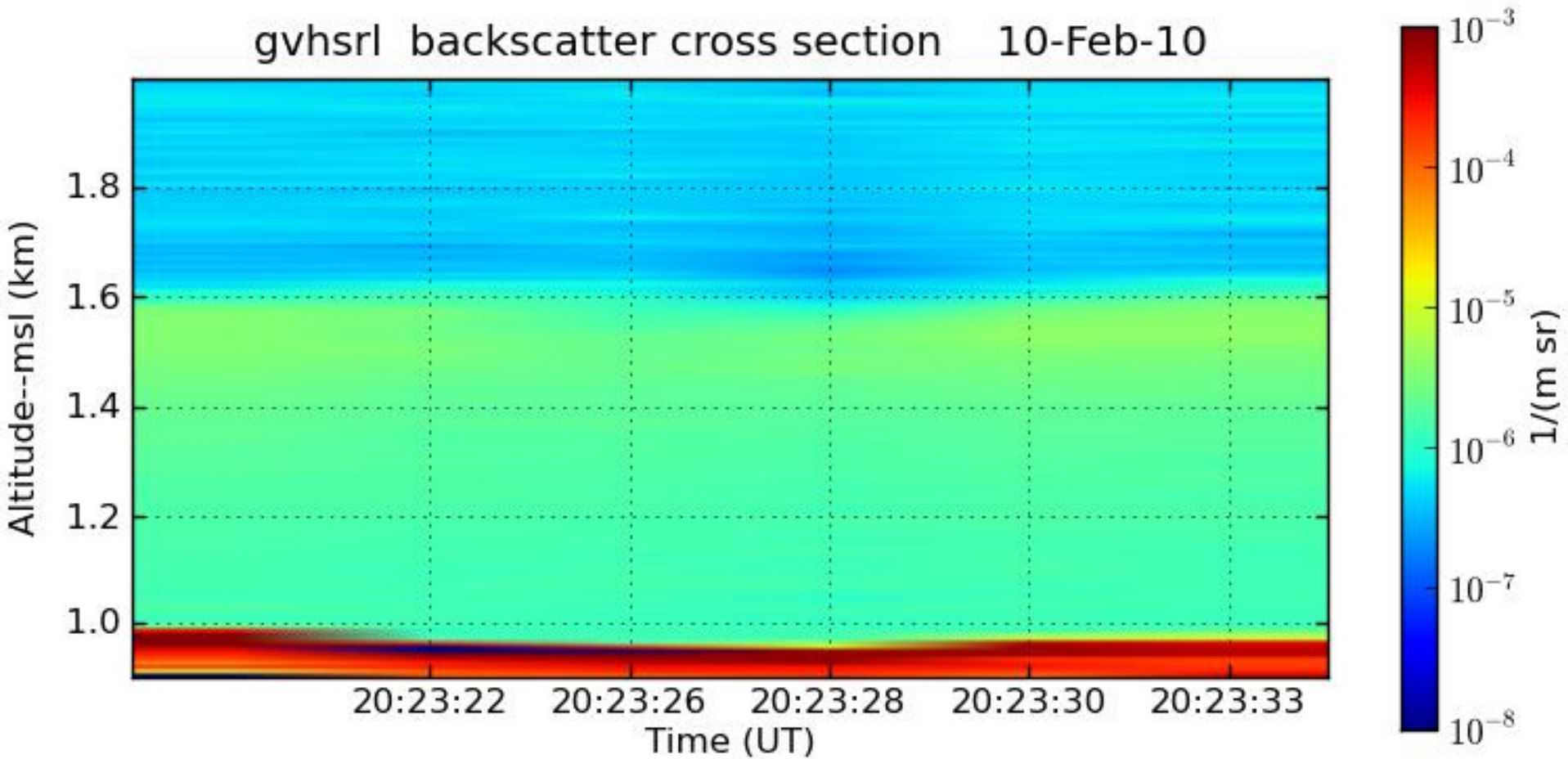
Particulate circular depolarization ratio(%) 10-Oct-2005

YEU-20051010-1200

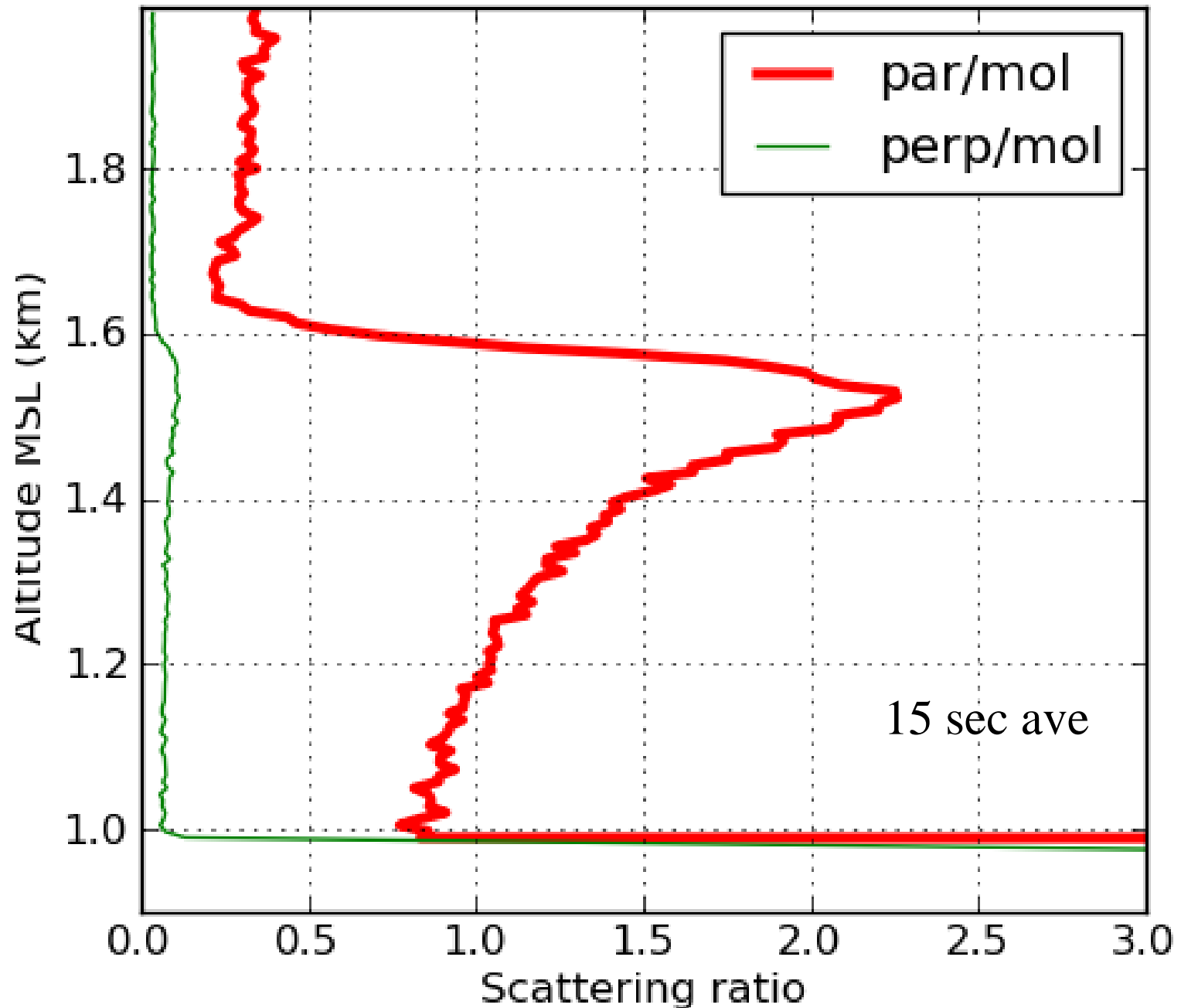


15-second observation of the the boundary layer

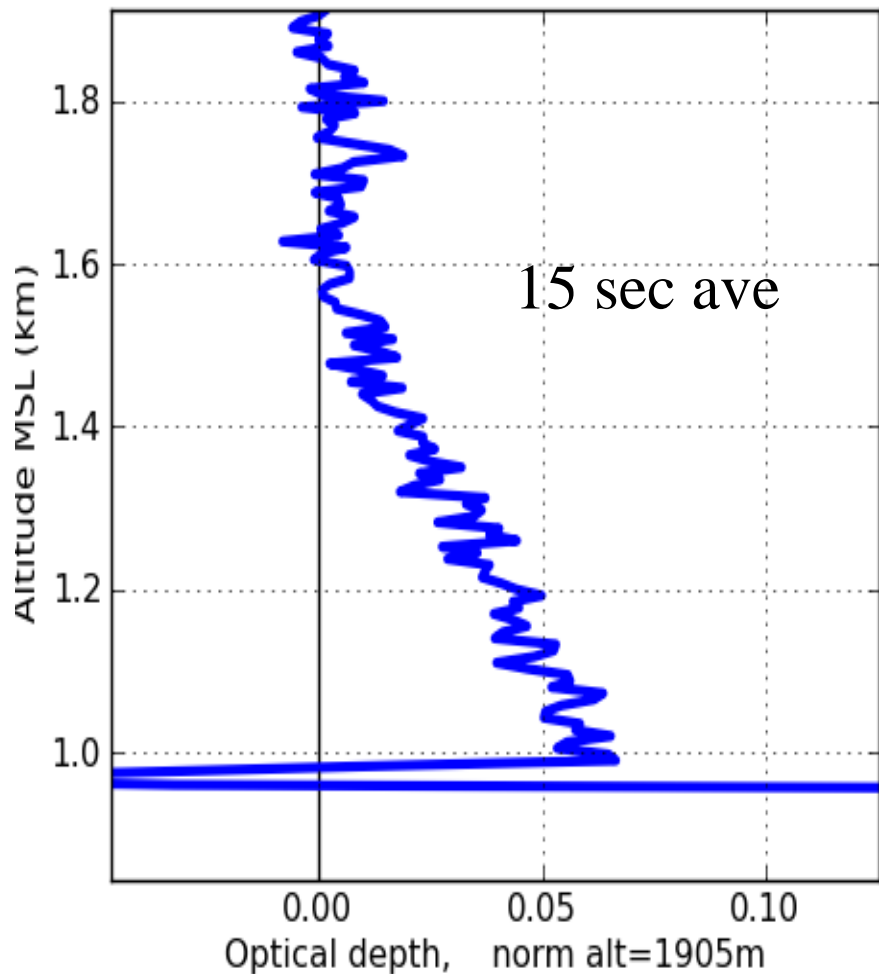
gvhsrl backscatter cross section 10-Feb-10



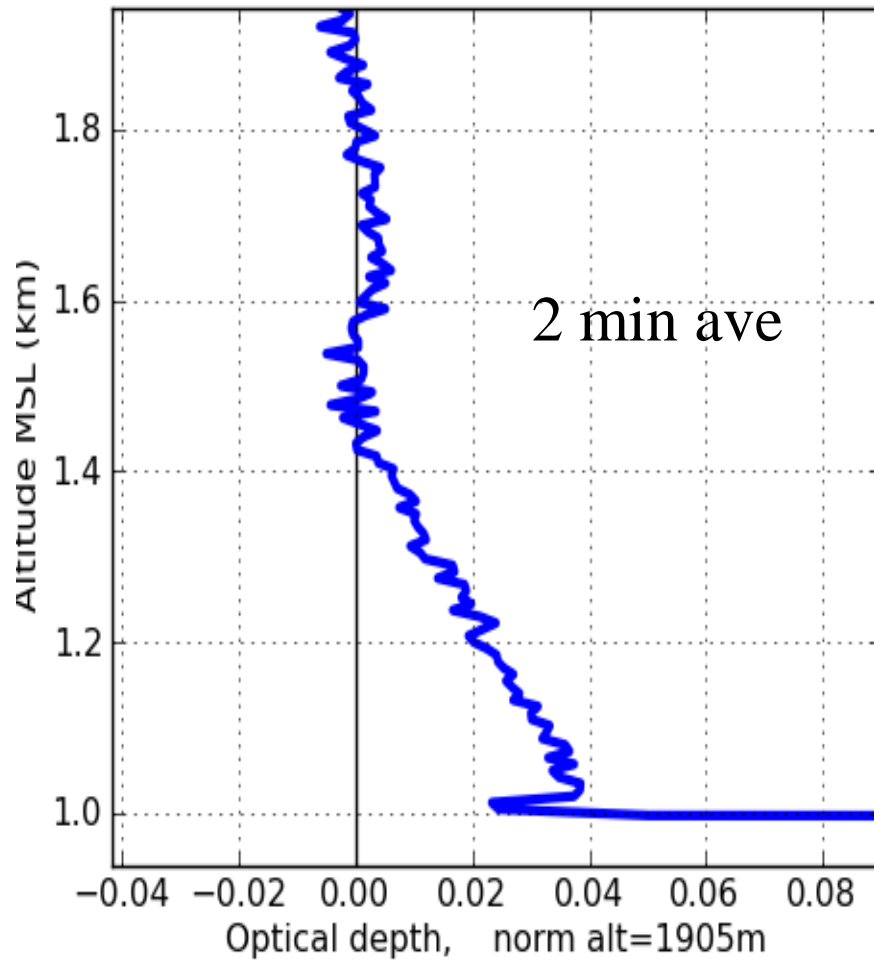
gvhsrl scat ratio 10-Feb-10 20:23-->20:23



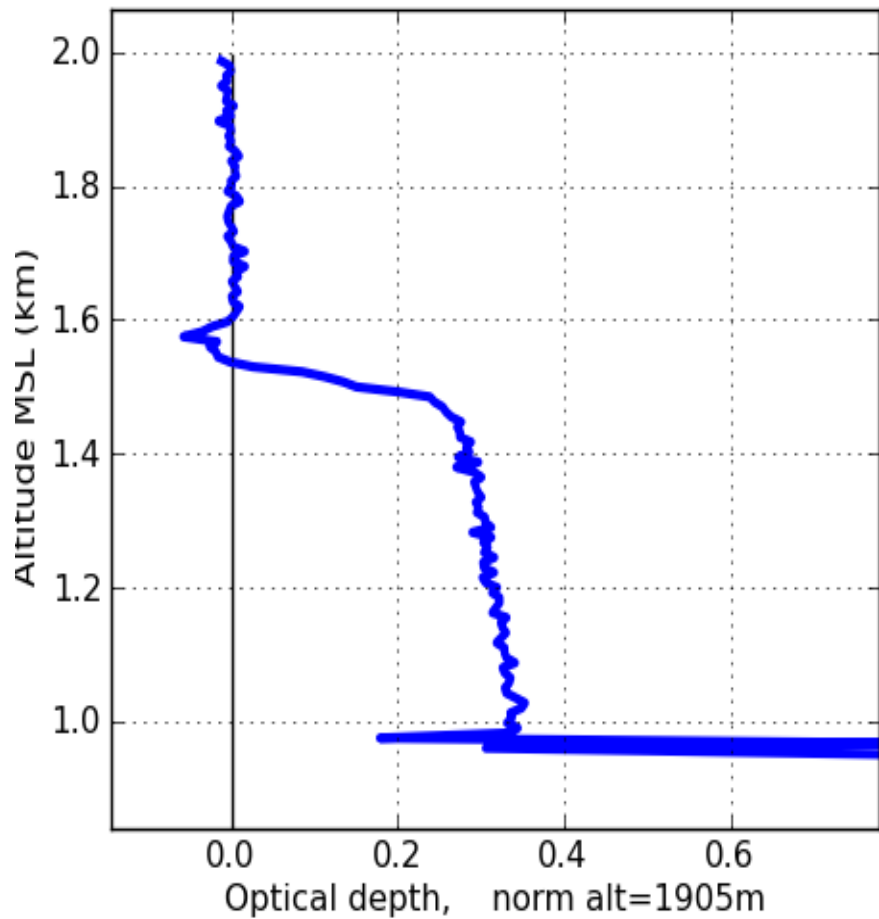
gvhsrl optical depth 10-Feb-10 20:23-->20:2



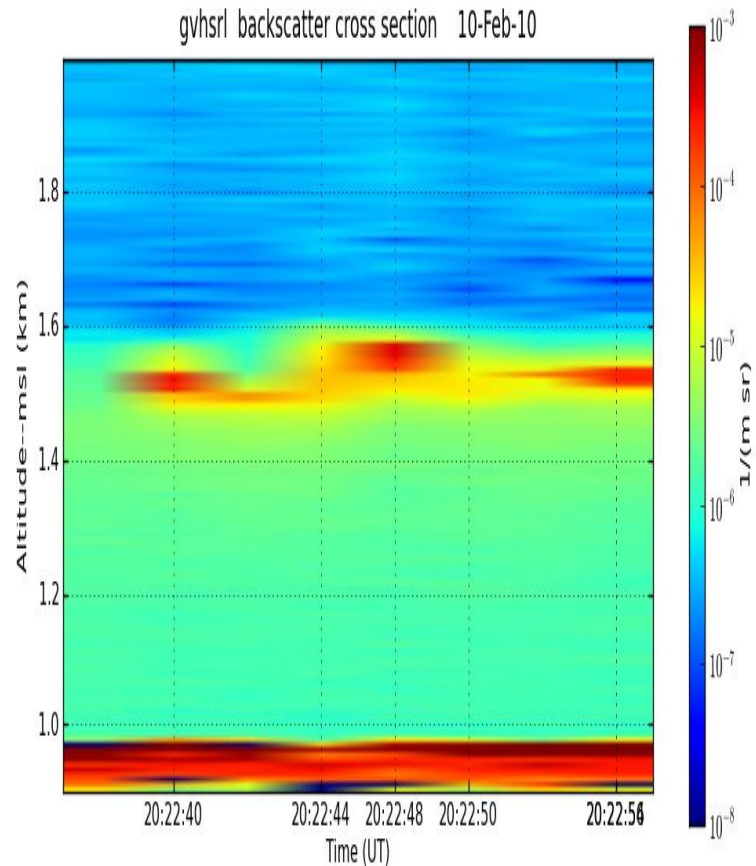
gvhsrl optical depth 10-Feb-10 20:23-->20:25



gvhsrl optical depth 10-Feb-10 20:22-->20:22

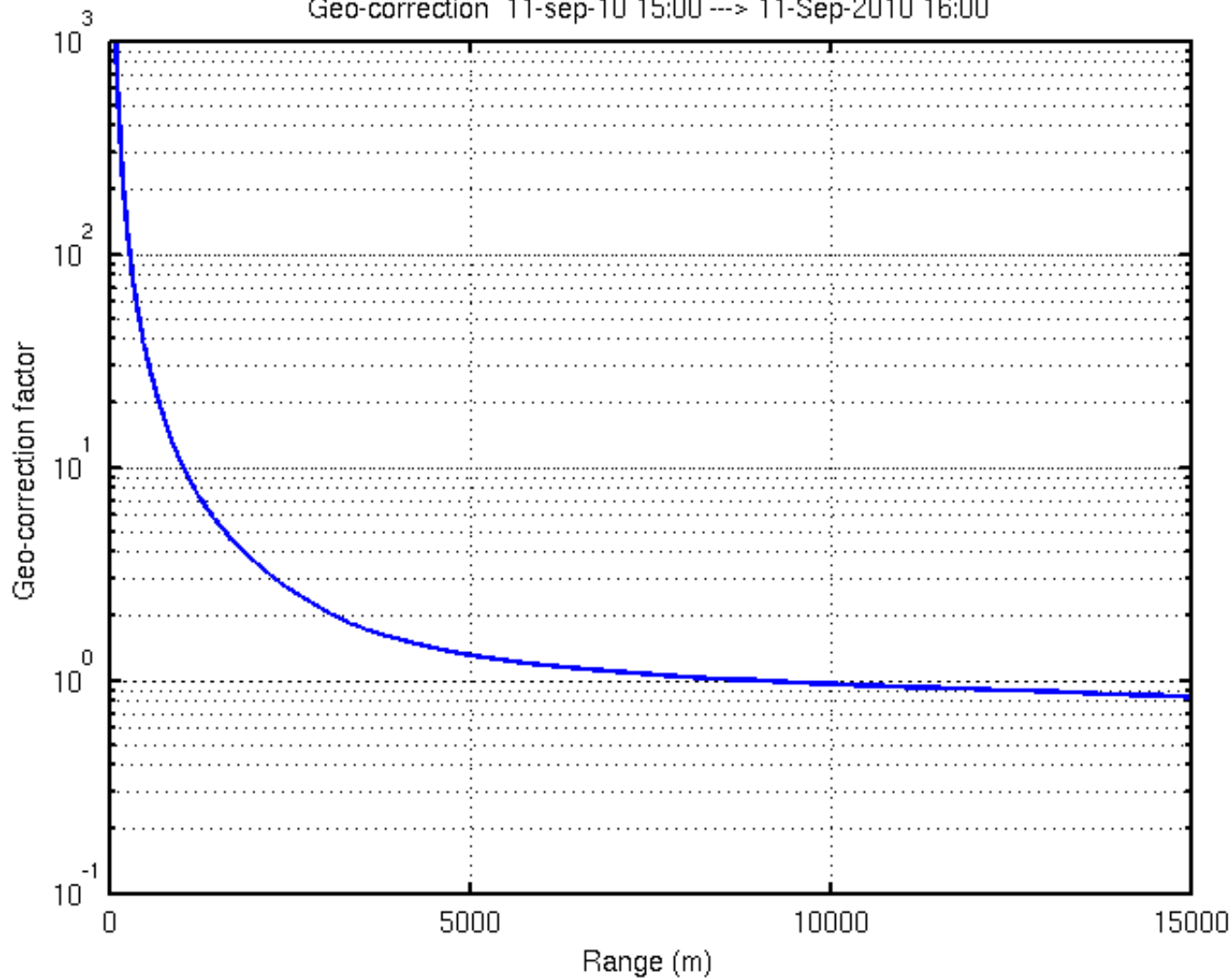


gvhsrl backscatter cross section 10-Feb-10

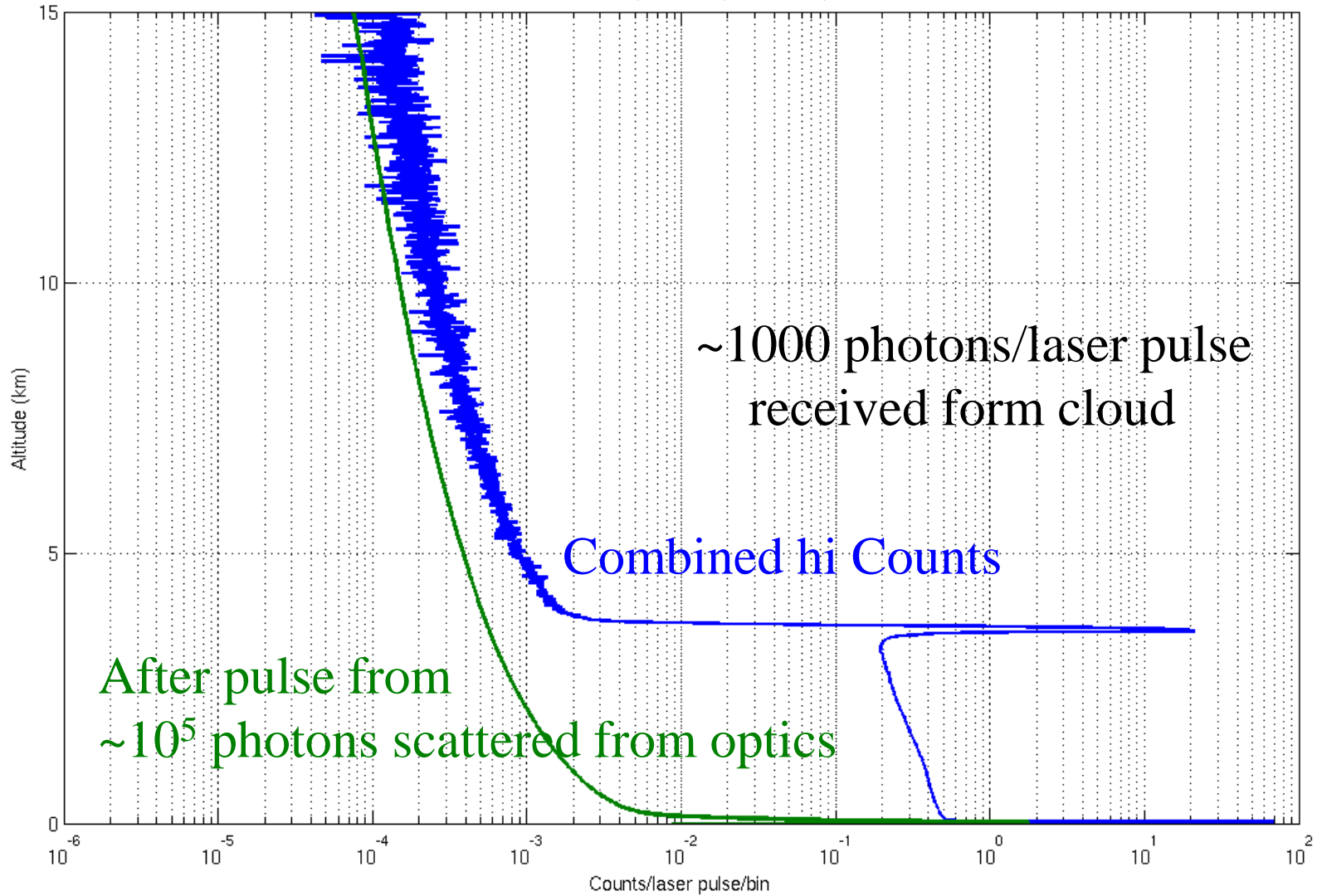


Optical depth profile for thin water cloud, 20 sec average

Geo-correction 11-sep-10 15:00 --> 11-Sep-2010 16:00



Aerosol return and laser pulse afterpulse 11-sep-10 3:30 UT

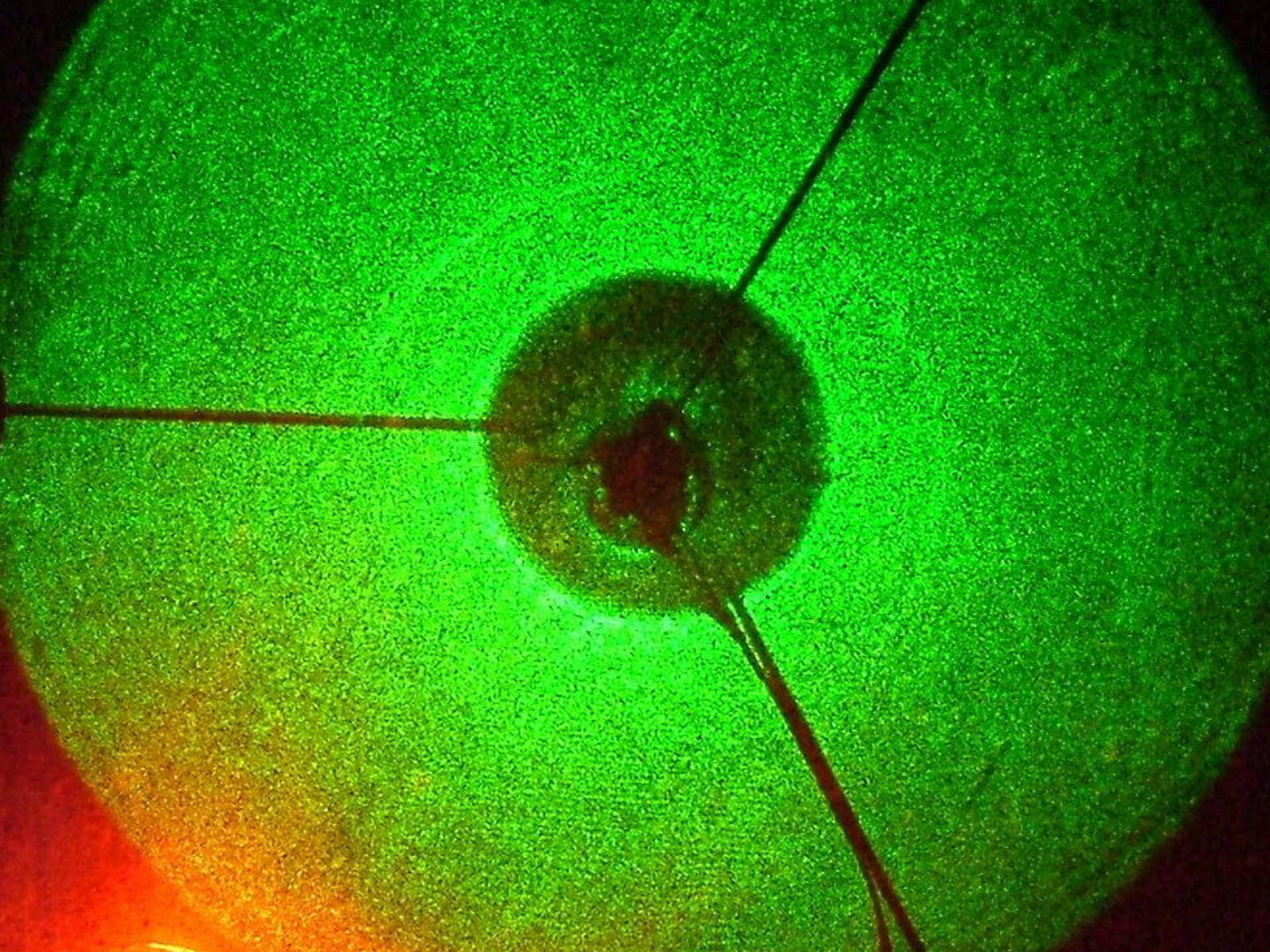


Advantages of 532 nm operation

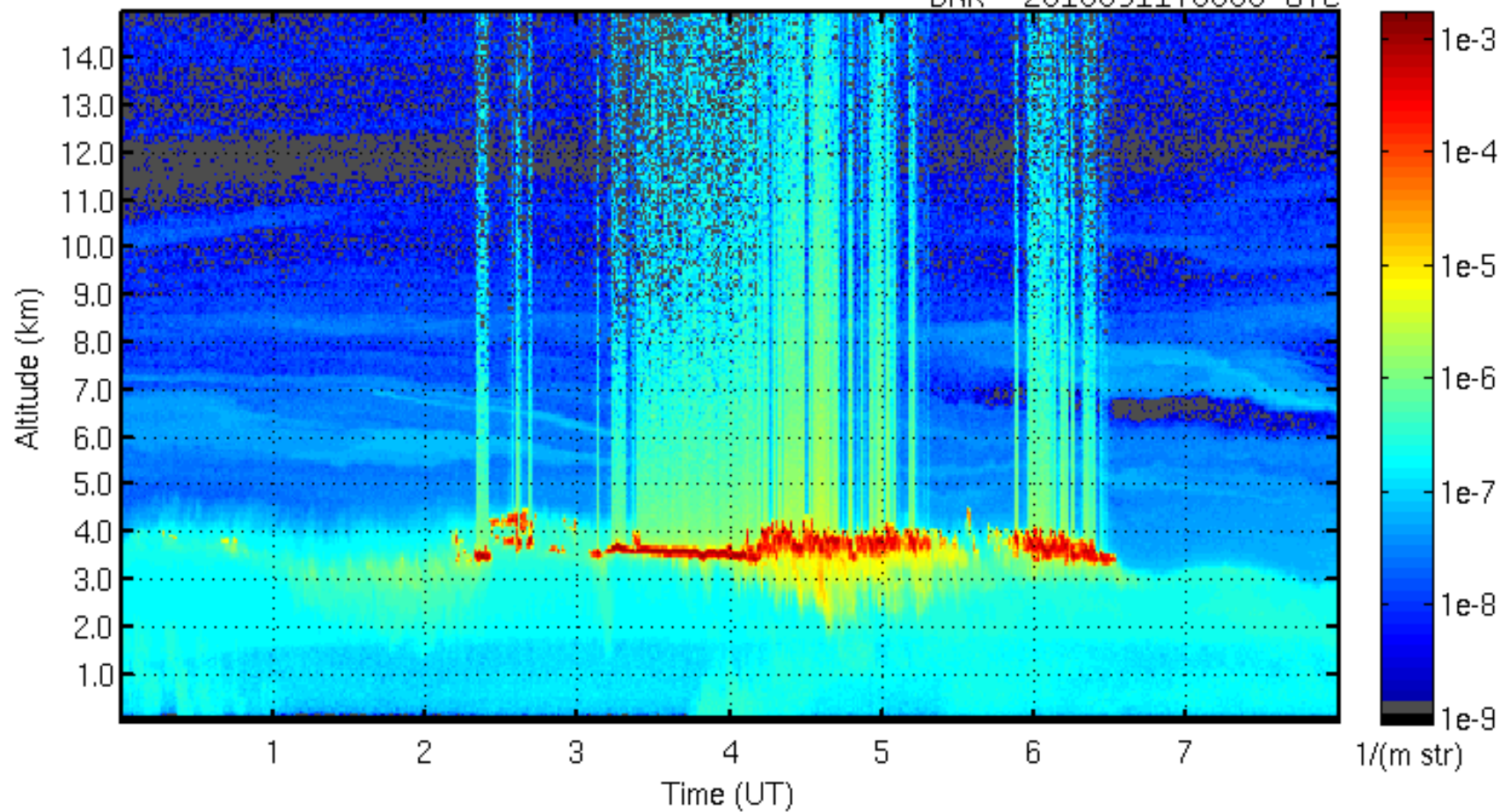
- Iodine adsorption line for filtering
- Important wavelength for radiative transfer
- Allows use of doubled Nd:YAG laser
- Strong molecular scattering

Problem with 532 nm—eye safety

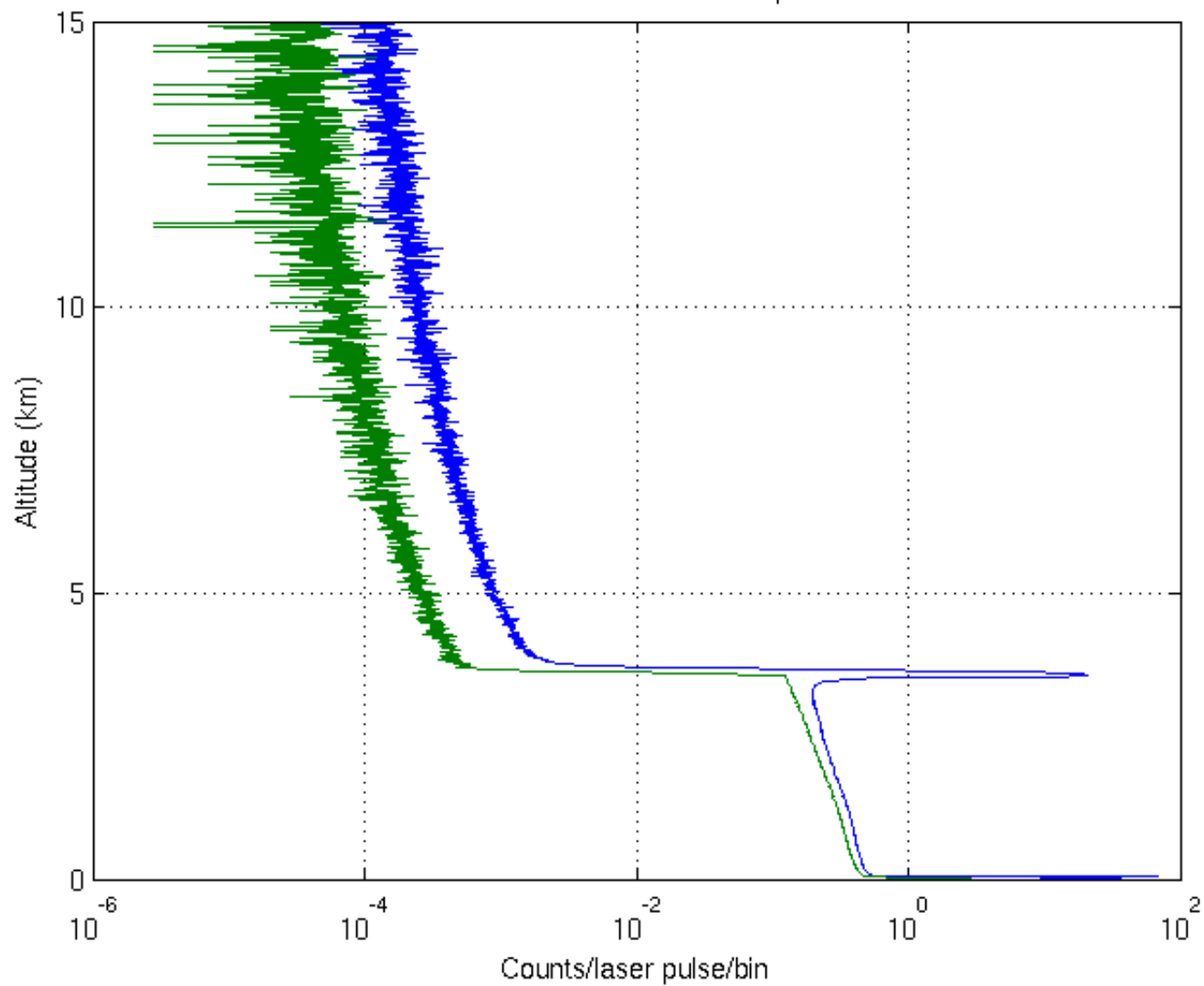
- Wavelength region with smallest permitted exposure
max single pulse exposure = $5e-7$ J/cm²



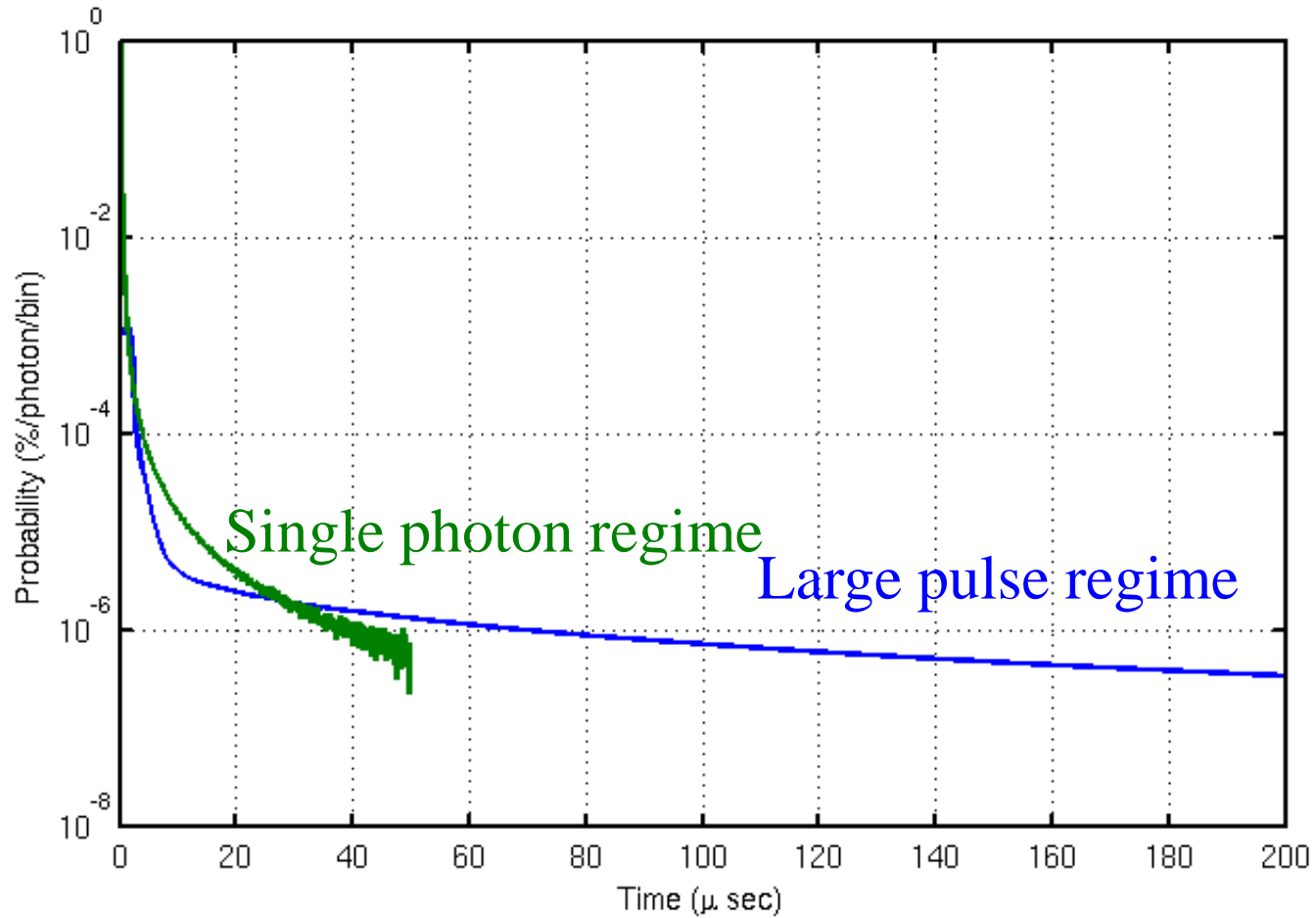
Aerosol backscatter cross section 11-Sep-2010
DNR 20100911T0000 UTC



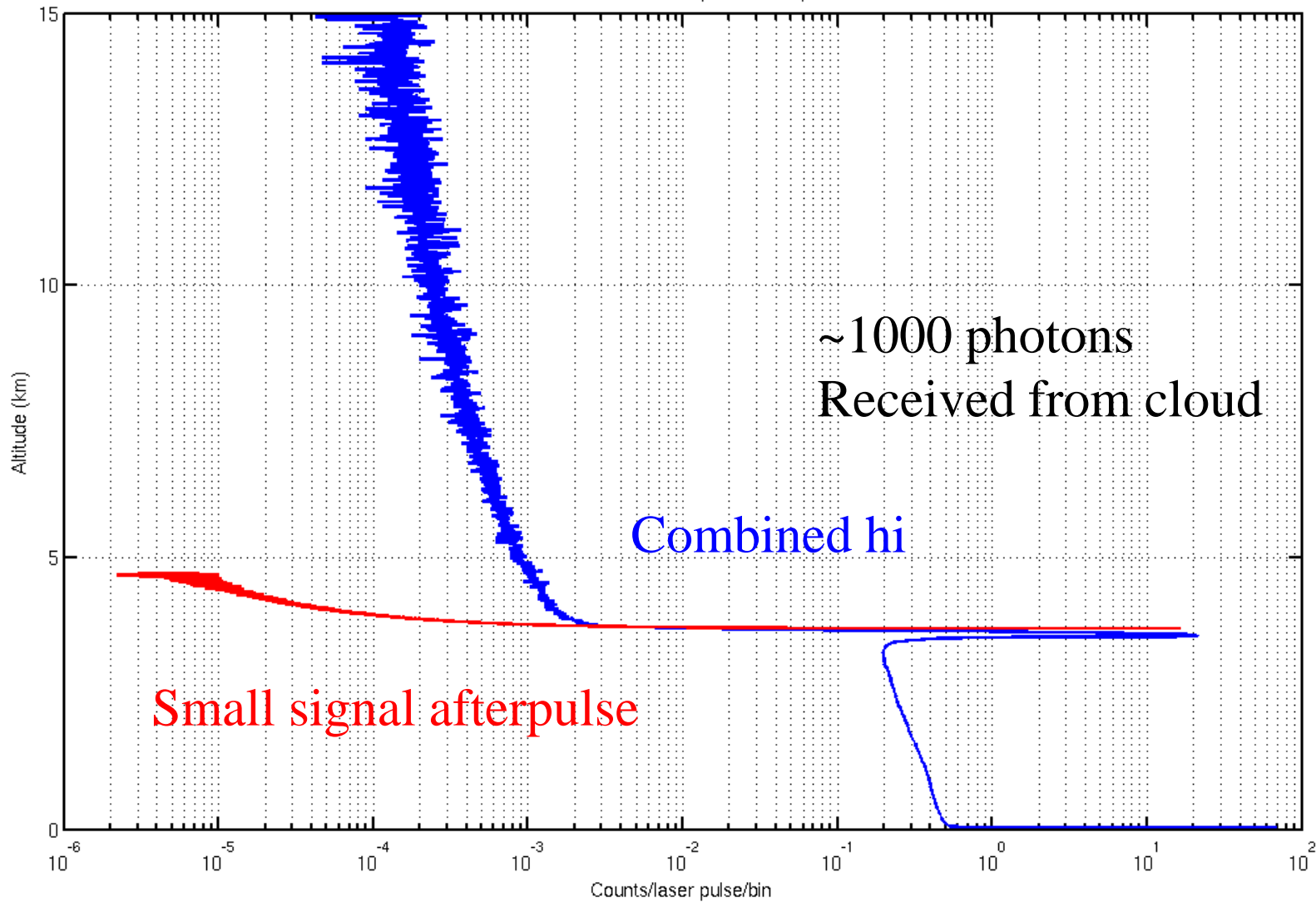
Aerosol and molecular returns 11-sep-10 3:30 UT

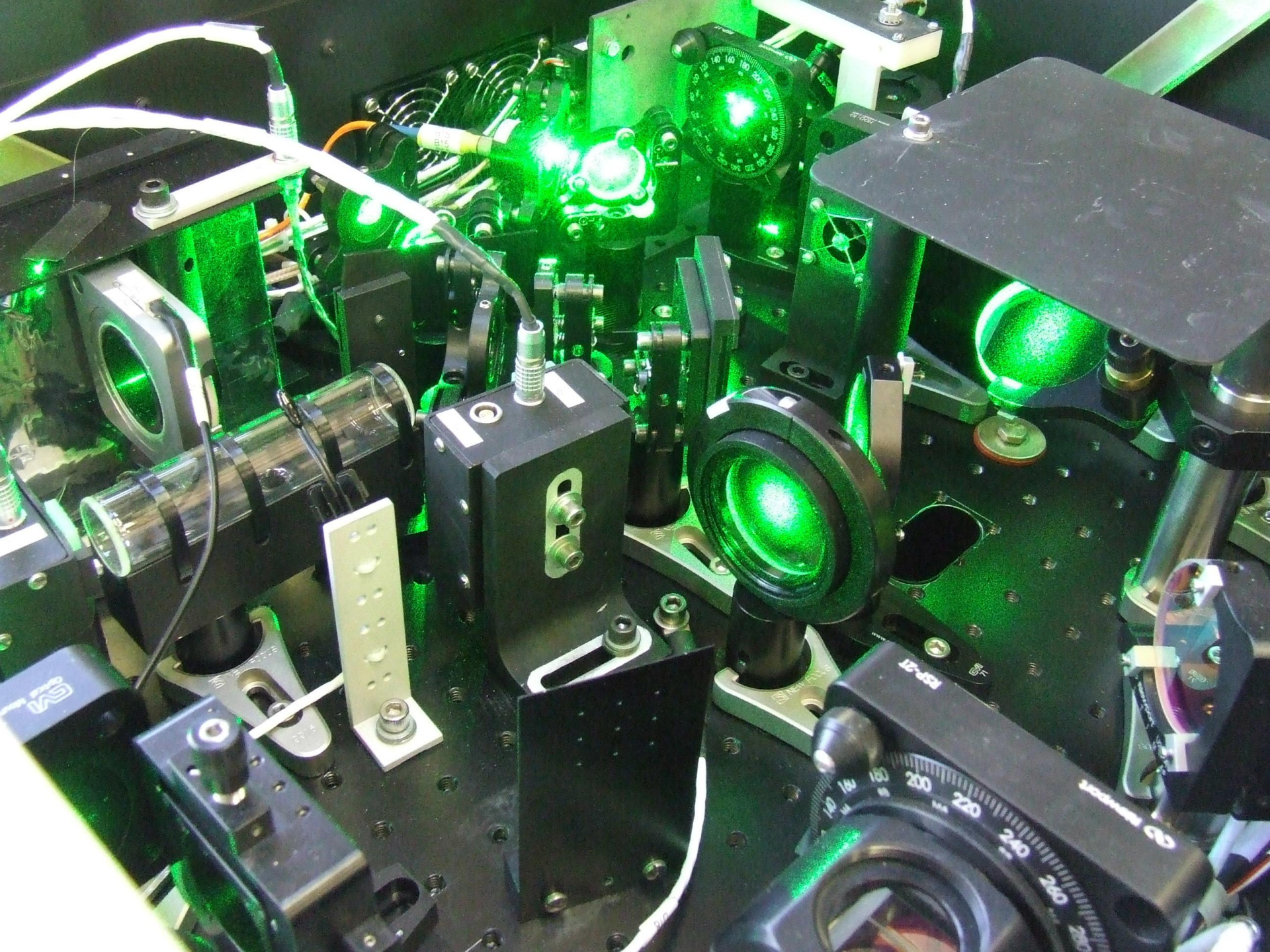


Geiger-mode APD afterpulse probability

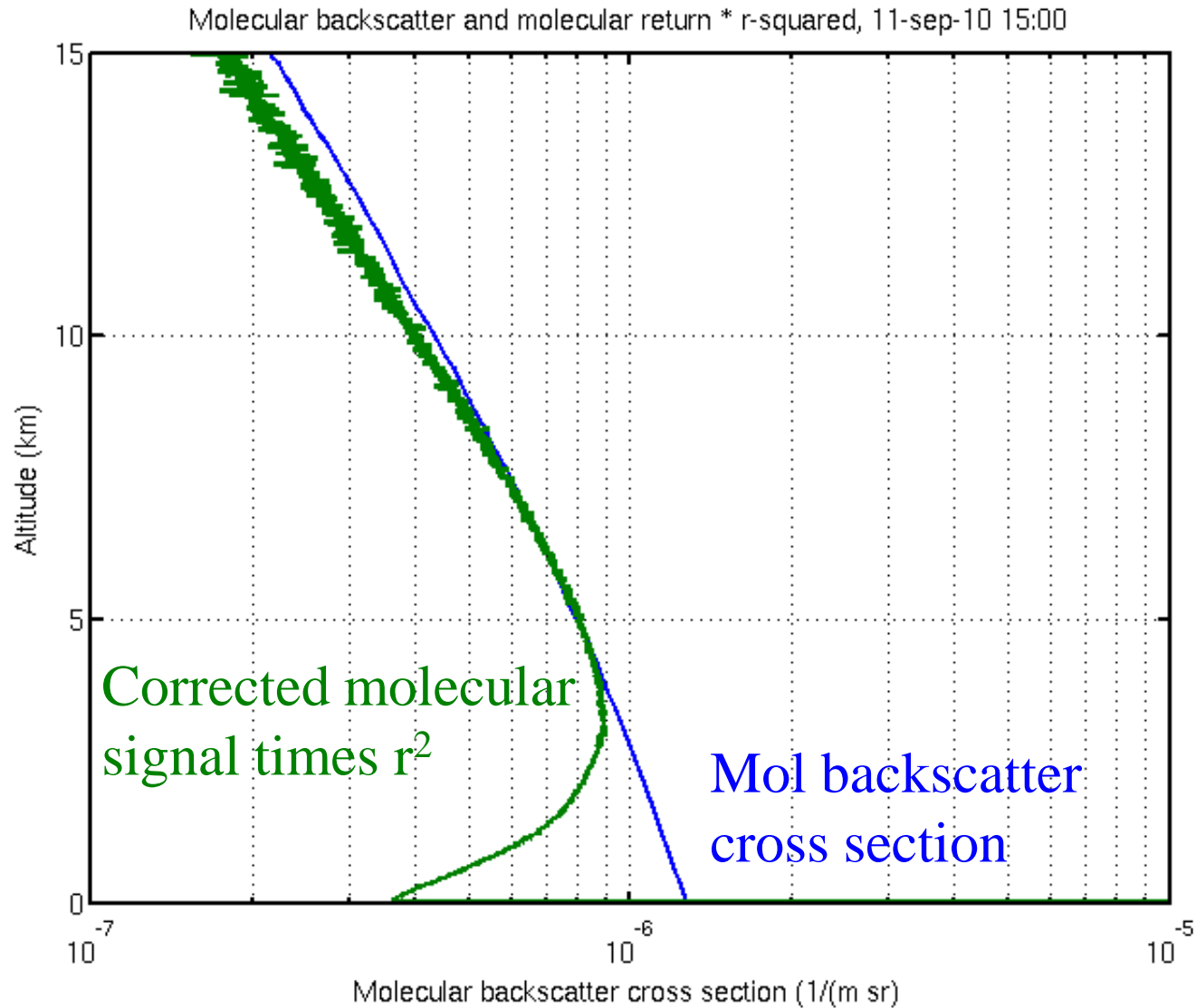


Aerosol return and cloud afterpulse 11-sep-10 3:30 UT

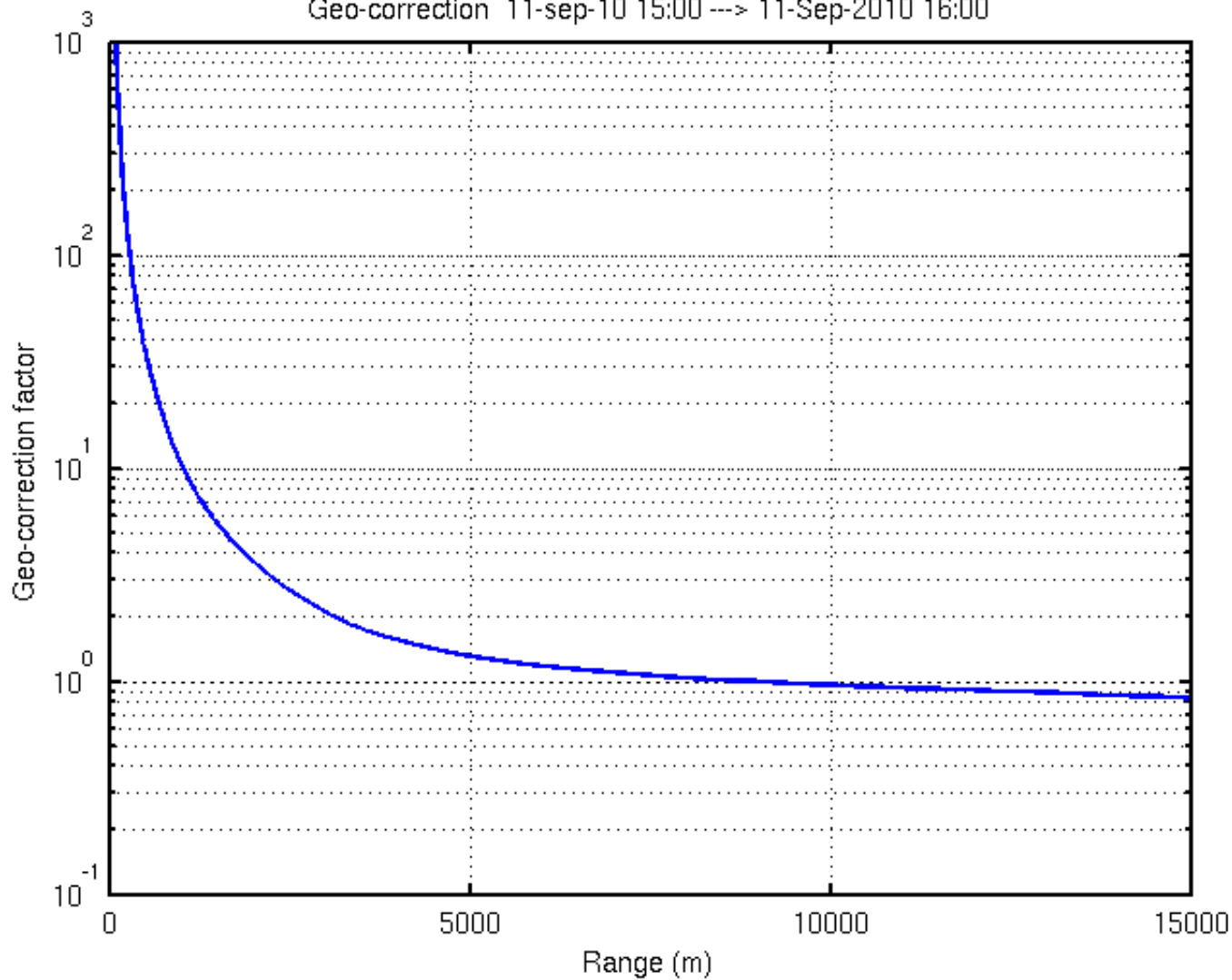




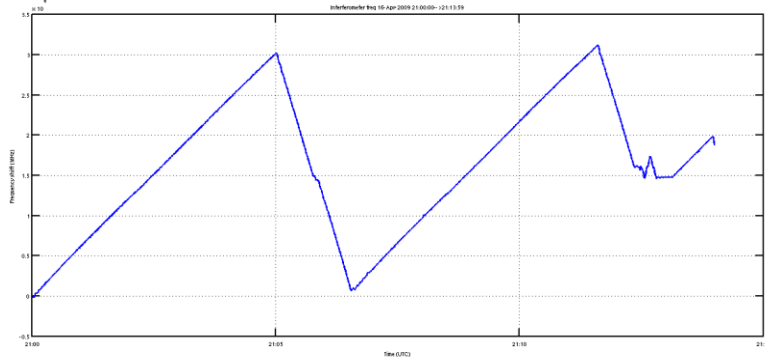
As the laser pulse propagates away from system the image size on the detector changes



Geo-correction 11-sep-10 15:00 --> 11-Sep-2010 16:00

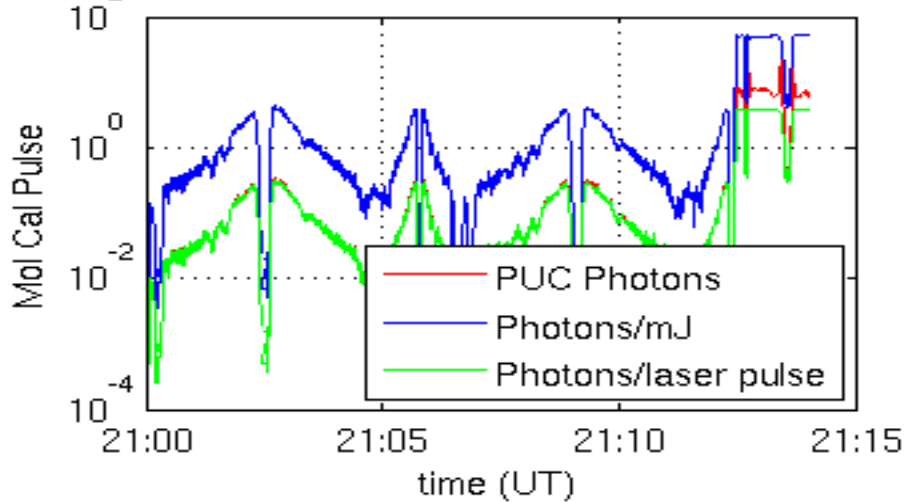


Receiver bandpass calibration

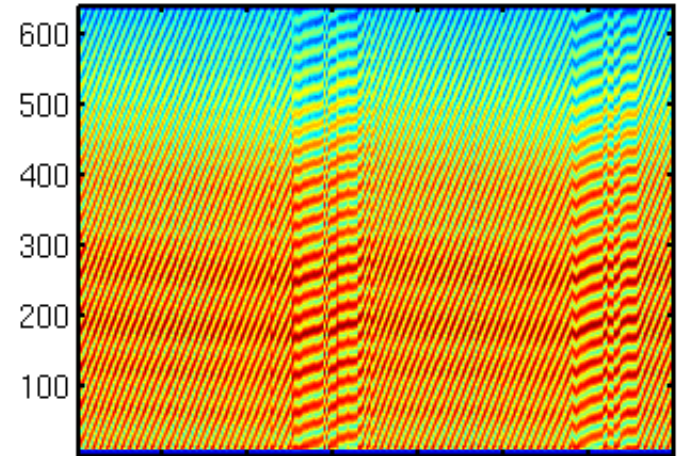


Frequency

Molecular cal pulse 16-Apr-2009 21:00:00-->21:13:59



Interferometer 16-Apr-2009 21:00:00-->16-Apr-2009 21:15

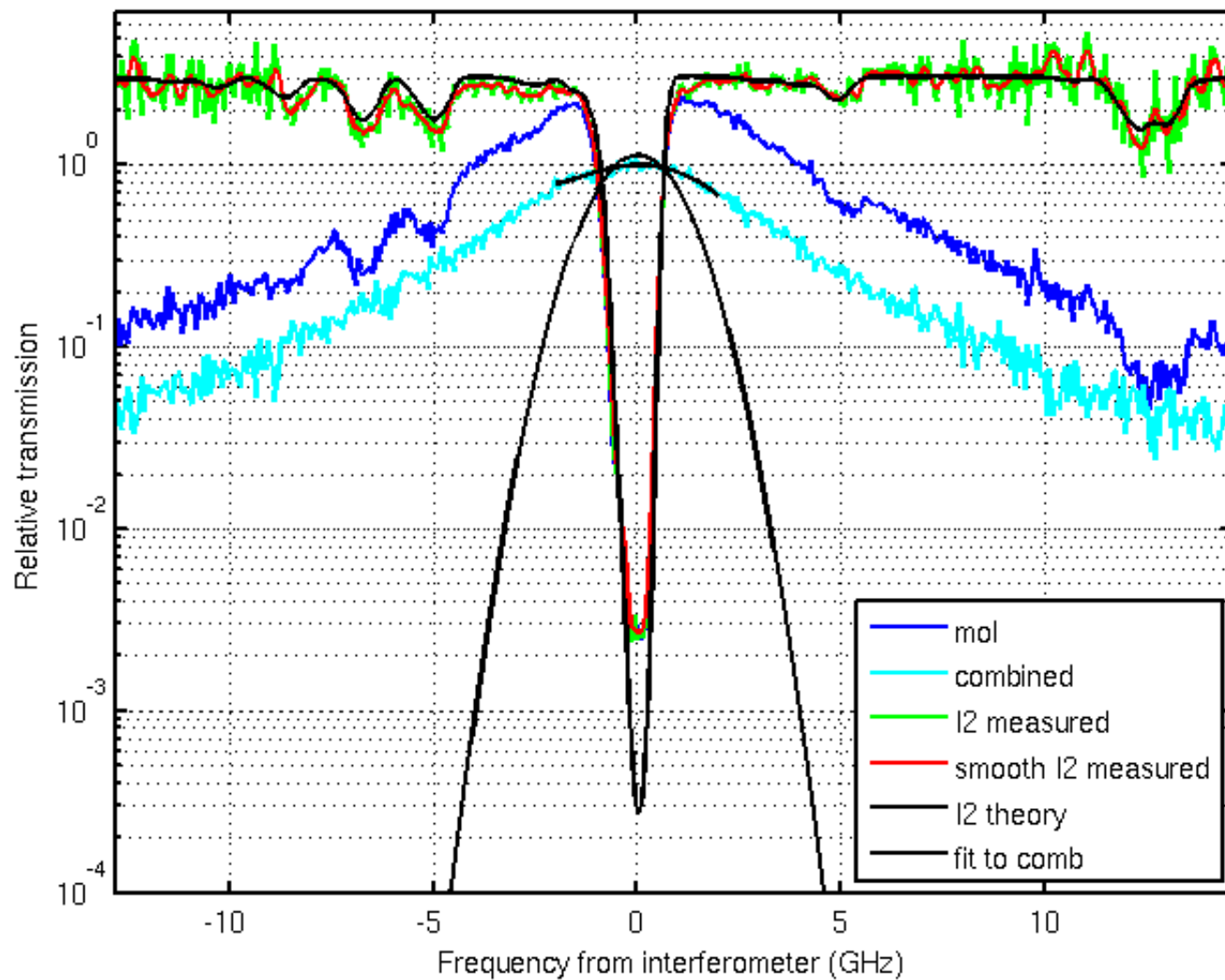


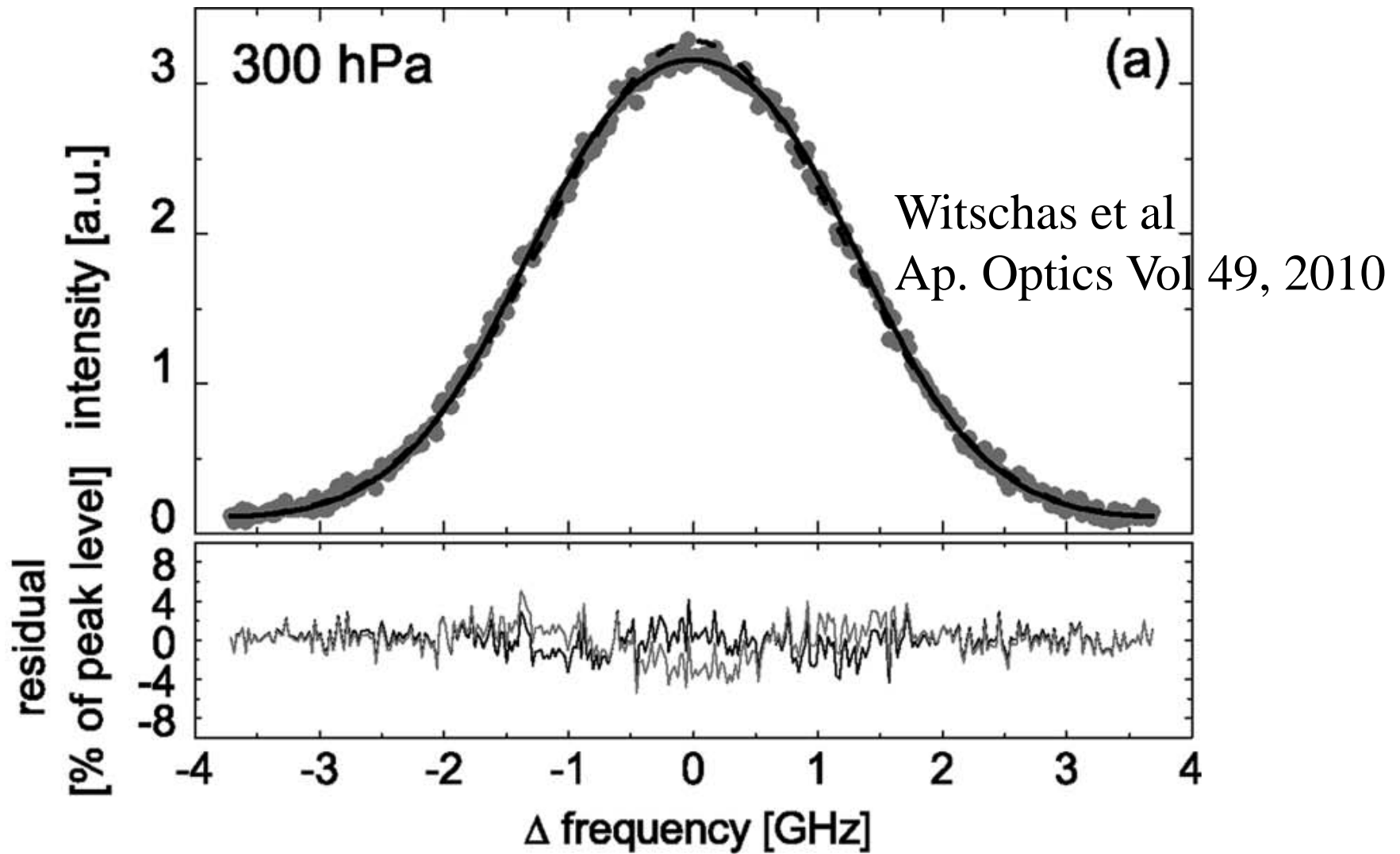
21:02 21:04 21:06 21:08 21:10 21:12

The transmitter frequency is scanned over ~ 20 GHz to measure the spectral bandpass of the receiver

An interferometer is used to determine frequency during the spectral scan

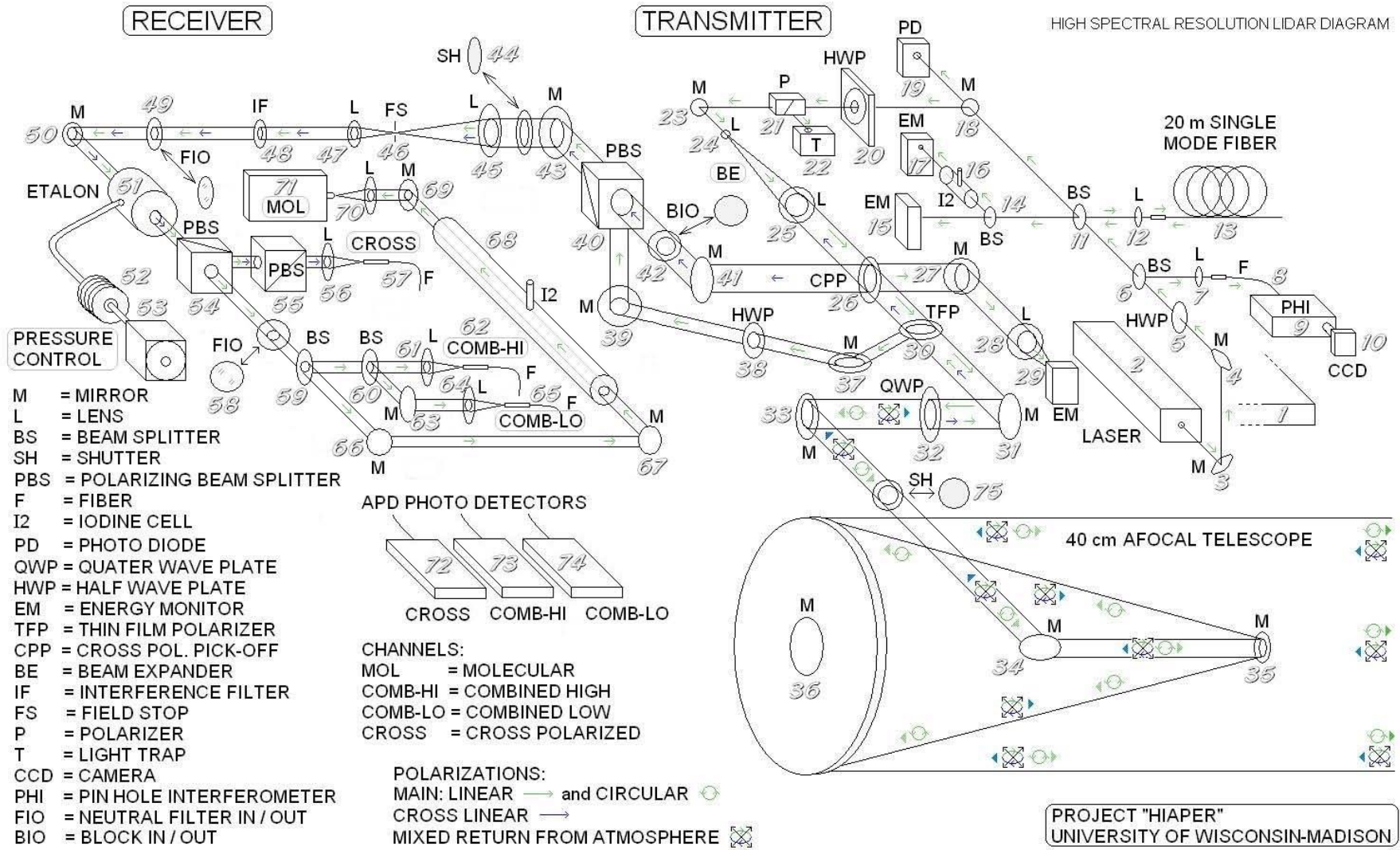
Completed Cal scan using interferometer freq ref 16-Apr-2009 20:59:00



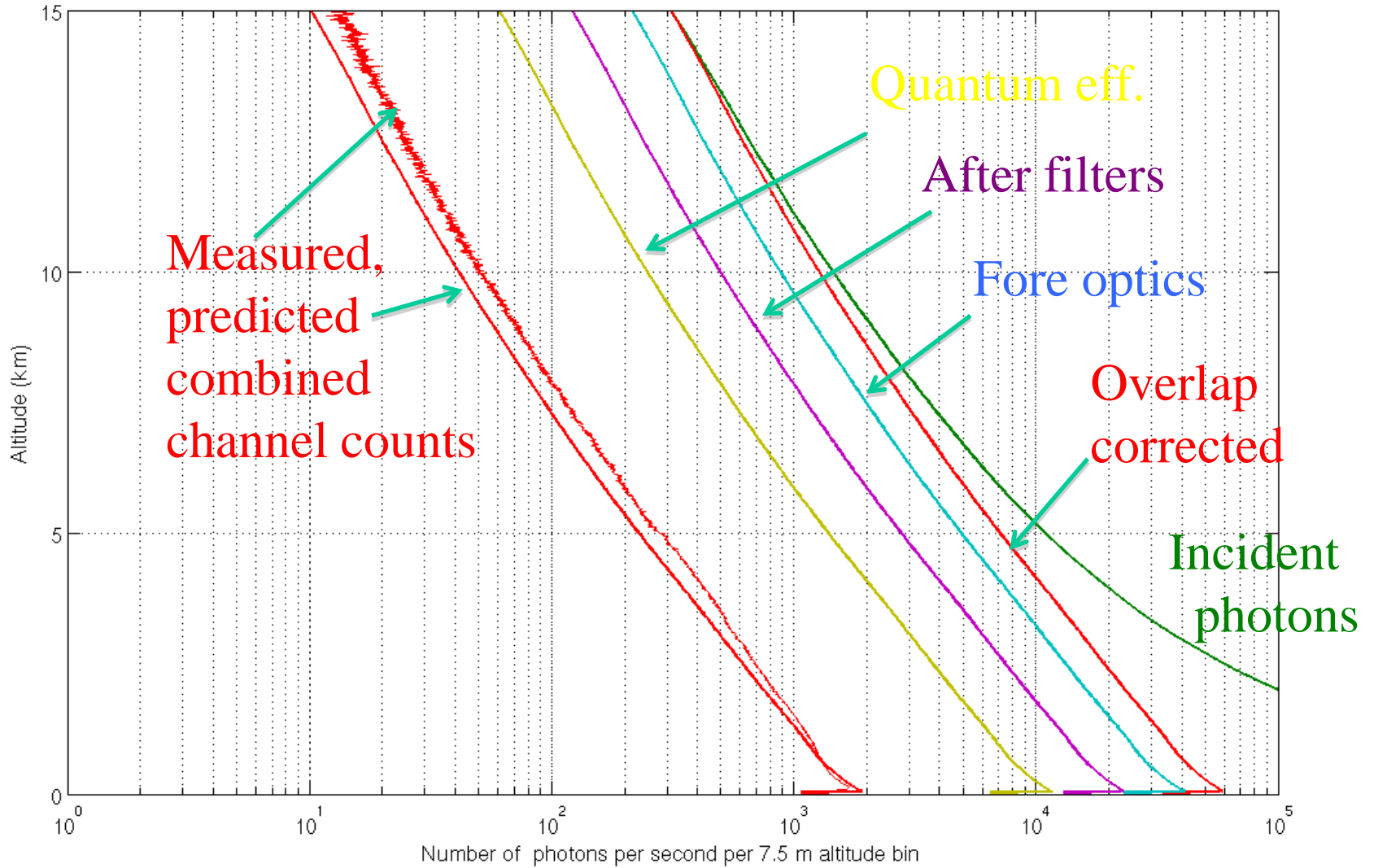


Brillouin line shape at 1000 hPa (solid), Rayleigh line shape (dashed) and deviations from measured values using Tenti S6 and Rayleigh shapes

HSRL schematic – NCAR HAIPER version



Predicted counts computed for clear air on 11-Sep-2010 14:00:00



Basic HSRL Equations

$$S_c = G_{ac}N_a + G_{mc}N_m ; \text{ eq 1—Signal in the combined channel}$$

$$S_m = G_{am}N_a + G_{mm}N_m ; \text{ eq 2—Signal in the molecular channel}$$

Where G_{ik} are gains of the two channels when exposed to N_a aerosol and N_m molecular photons.

Solving for N_m and N_a yields:

$$N_m = \frac{S_m/G_{am} - S_c/G_{ac}}{(G_{mm}/G_{am}) - (G_{mc}/G_{ac})}; \text{ eq 3—Number of molecular photons incident as function of signals}$$

$$N_a = \frac{S_c/G_{mc} - S_m/G_{mm}}{(G_{ac}/G_{mc}) - (G_{am}/G_{mm})}; \text{ eq 4 Number of aerosol photons incident as function of signals}$$

With G_{ac} = gain of the combined channel when exposed to aerosol photons

Define other gains relative to G_{ac} :

$$G_{mc} = C_{mc} \cdot G_{ac}, G_{am} = C_{am} \cdot G_{ac}, G_{mm} = C_{mm} \cdot G_{ac}$$

$$N_m = (1/G_{ac}) \cdot \frac{S_m/C_{am} - S_c}{(C_{mm}/C_{am}) - C_{mc}} = (1/G_{ac}) \cdot \frac{S_m - C_{am} S_c}{C_{mm} - C_{mc} C_{am}}$$

$$N_a = (1/G_{ac}) \cdot \frac{S_c/C_{mc} - S_m/C_{mm}}{(1/C_{mc}) - (C_{am}/C_{mm})} = (1/G_{ac}) \cdot \frac{C_{mm} S_c - C_{mc} S_m}{C_{mm} - C_{mc} C_{am}}$$

The scattering ratio is then:

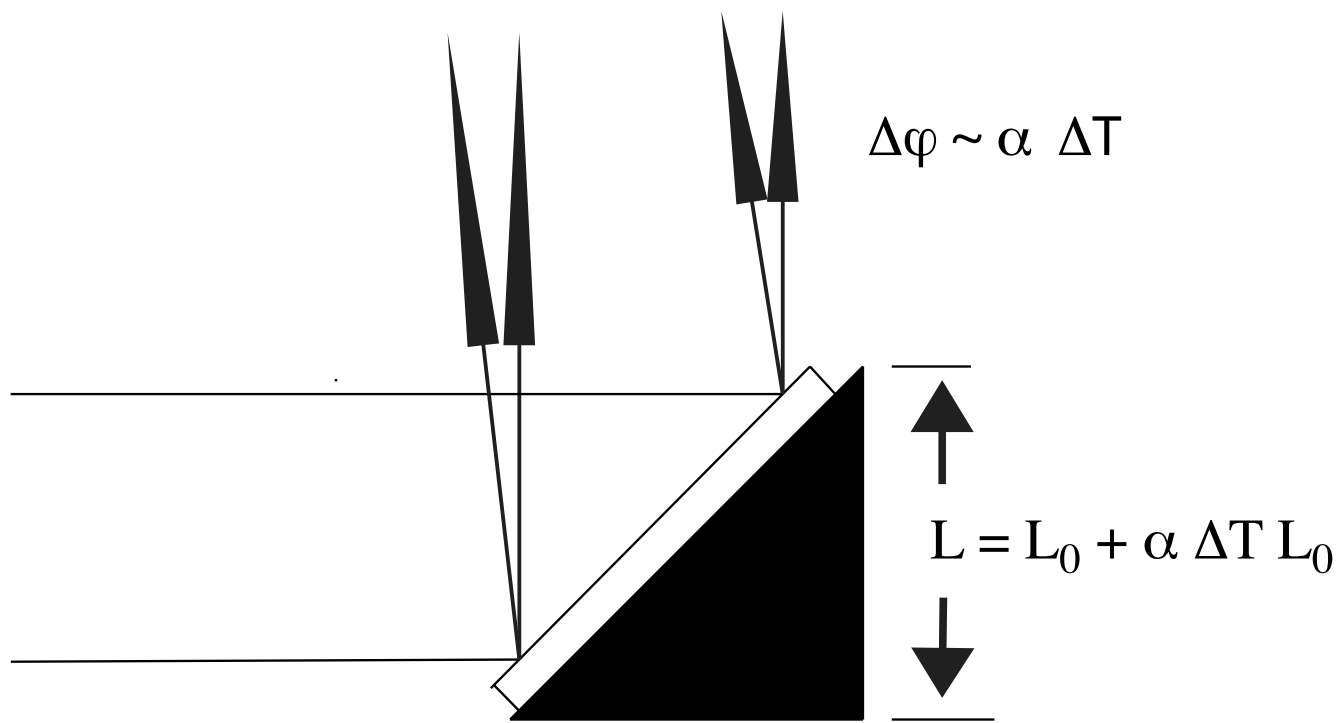
$$\frac{N_a}{N_m} = \frac{C_{mm} S_c - C_{mc} S_m}{S_m - C_{am} S_c}$$

The backscatter cross section, β'_a , is:

$$\beta'_a(r) = \beta_a(r) \cdot \frac{P(180,r)}{4\pi} = \frac{N_a(r)}{N_m(r)} \cdot \beta_m(r), \text{ where } \beta_a = \text{scattering cross section, } \frac{P(180,r)}{4\pi} = \text{backscatter phase function.}$$

the optical depth, τ , between two points r_1 and r_2 is:

$$\tau(r_2 - r_1) = \frac{1}{2} \cdot \log\left(\frac{r_1^2 \rho(r_2) \cdot N_m(r_1)}{r_2^2 \rho(r_1) \cdot N_m(r_2)}\right), \text{ where } \rho(r) = \text{the atmospheric density profile}$$



Thermal expansion of components effect the alignment of transmitter with the receiver. Here we consider the example of an 45 deg aluminum mountin block for a beam turning mirror.

Angle shift due to 10 deg C temperature change: $\Delta\varphi \sim \alpha \Delta T \sim 2.5 * 10^{-5} * 10$
 $\Delta\varphi \sim 250$ microradian

Problem with 532 nm—eye safety

--Wavelength region with smallest permitted exposure

$$\text{ANSI safe exposure} \leq 5e-7 (R/4)^{-1/4} \text{ J/cm}^2$$

Where R = the pulse repetition rate

This forces high repetition rate and large apertures

Range ambiguity limits $R < \sim 4\text{kHz}$, i.e. $r_{\text{max}} < \sim 40 \text{ km}$

Cost, complexity, turbulence limit aperture to $\sim 0.5 \text{ m}$.

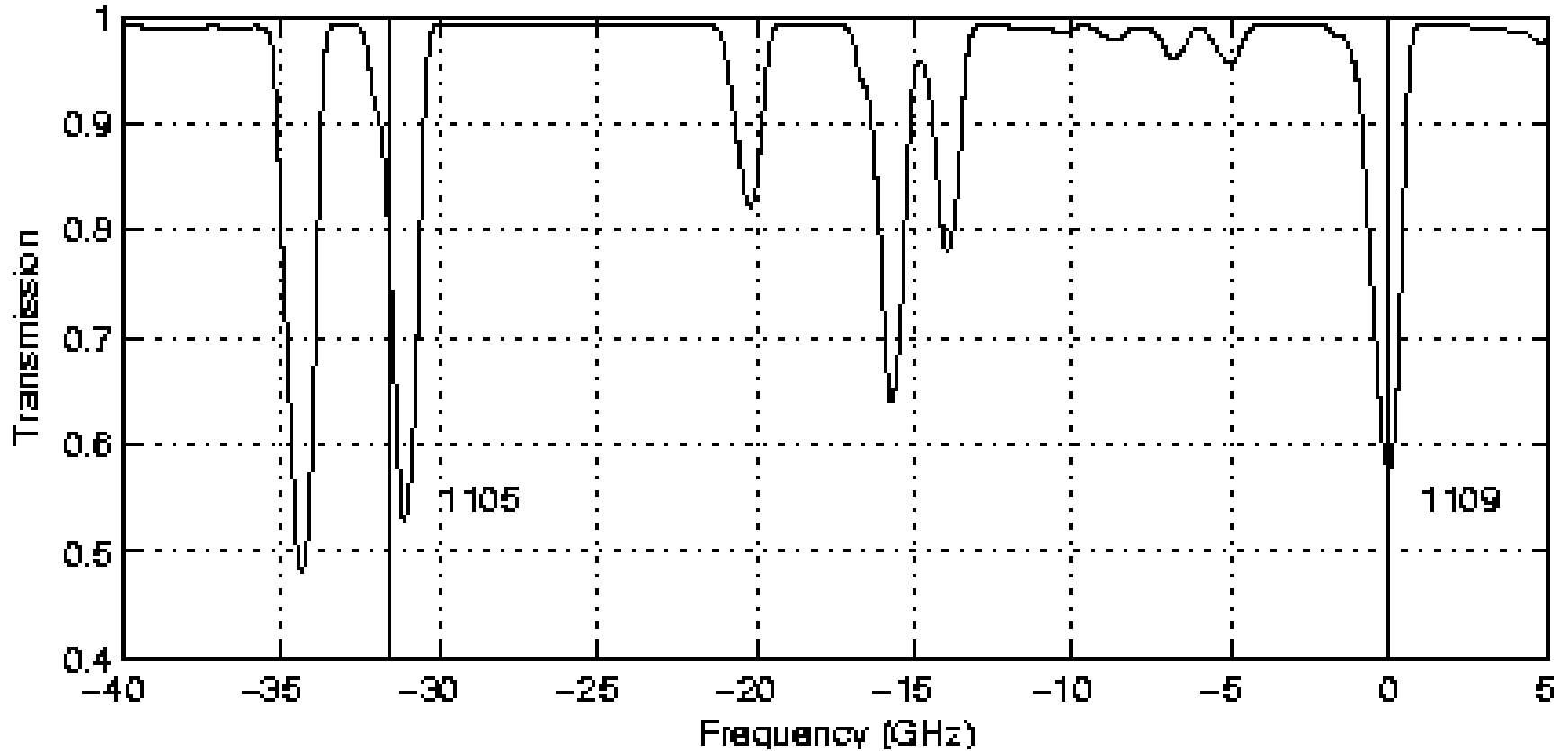
Thus max transmitted energy laser pulse is limited to:

$$\pi 25^2 * 5e-7 * 1000^{-1/4} = 0.174 \text{ mJ/pulse}$$

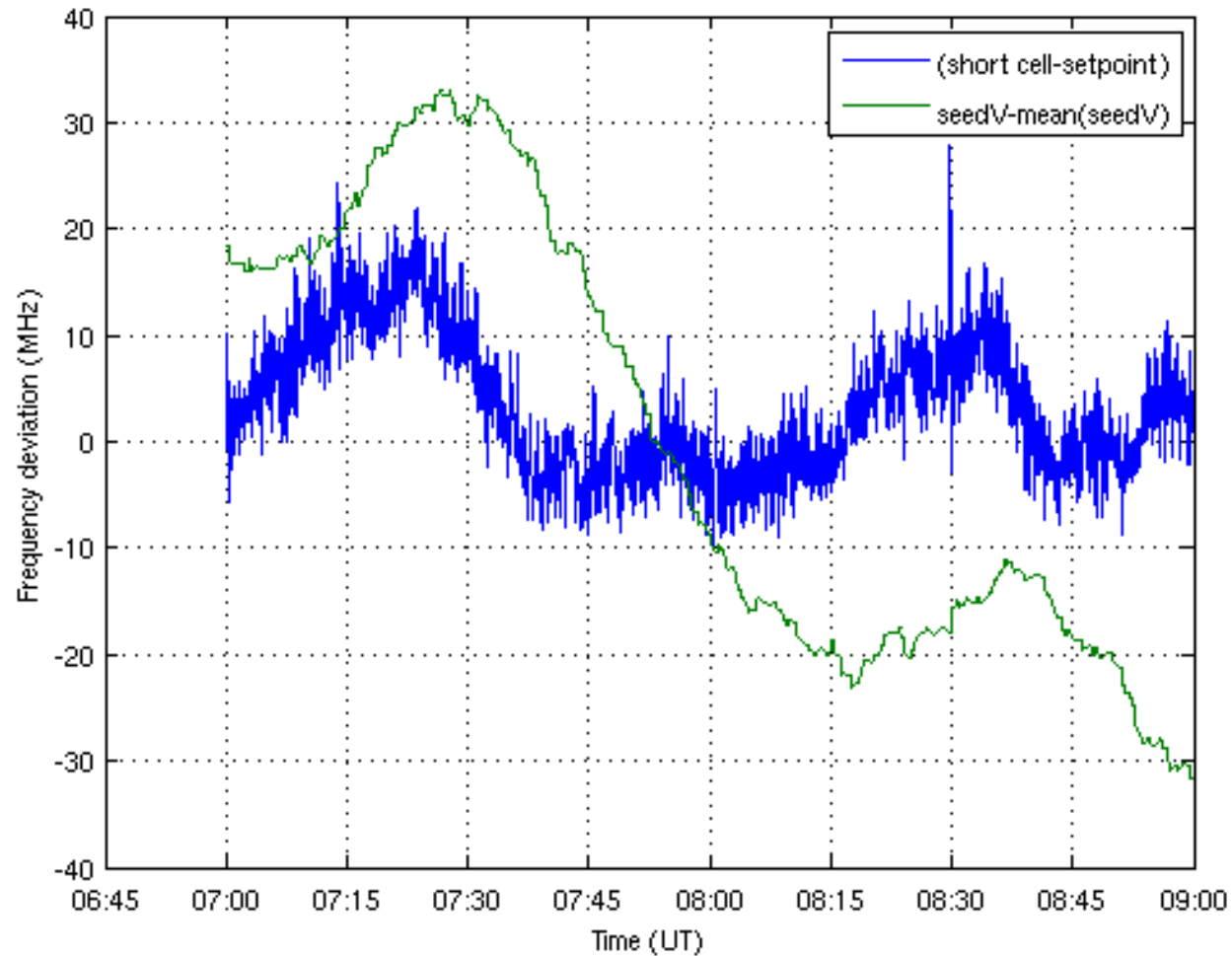
and the maximum transmitted power is:

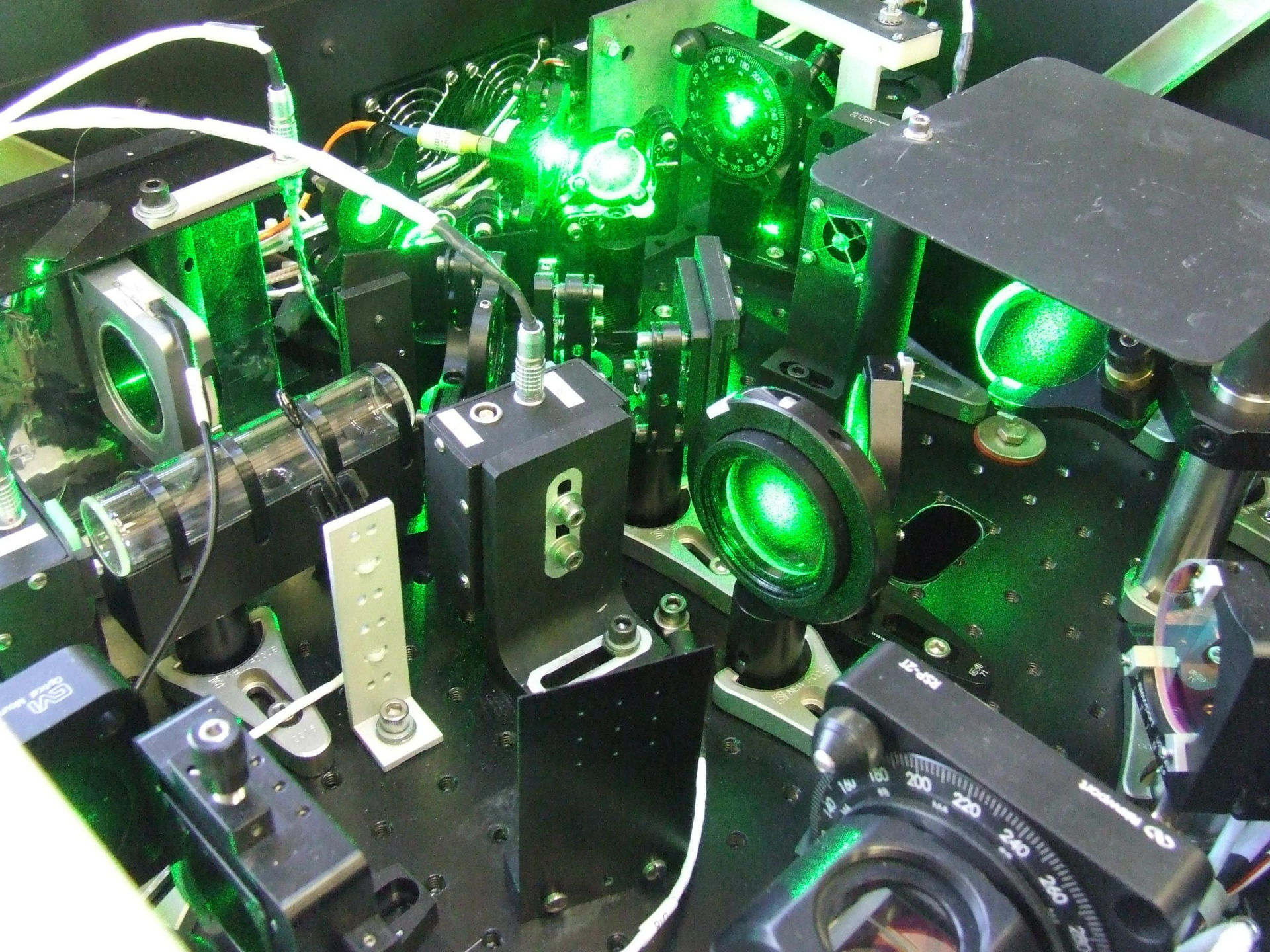
$$0.174e-3 * 4000 \text{ Hz} = 0.7 \text{ Watt}$$

Transmission of 2-cm iodine cell



Example of frequency locking





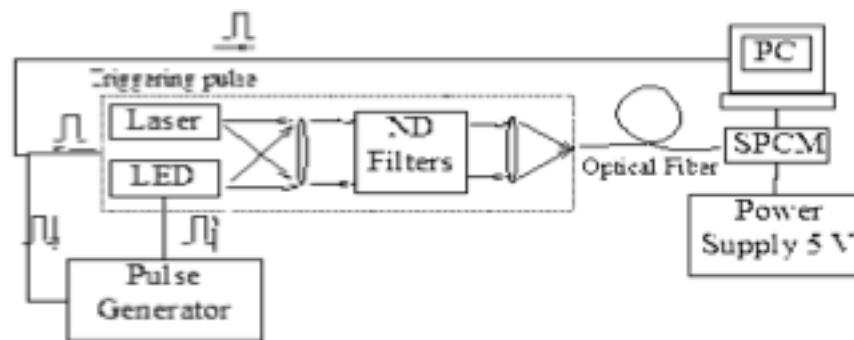
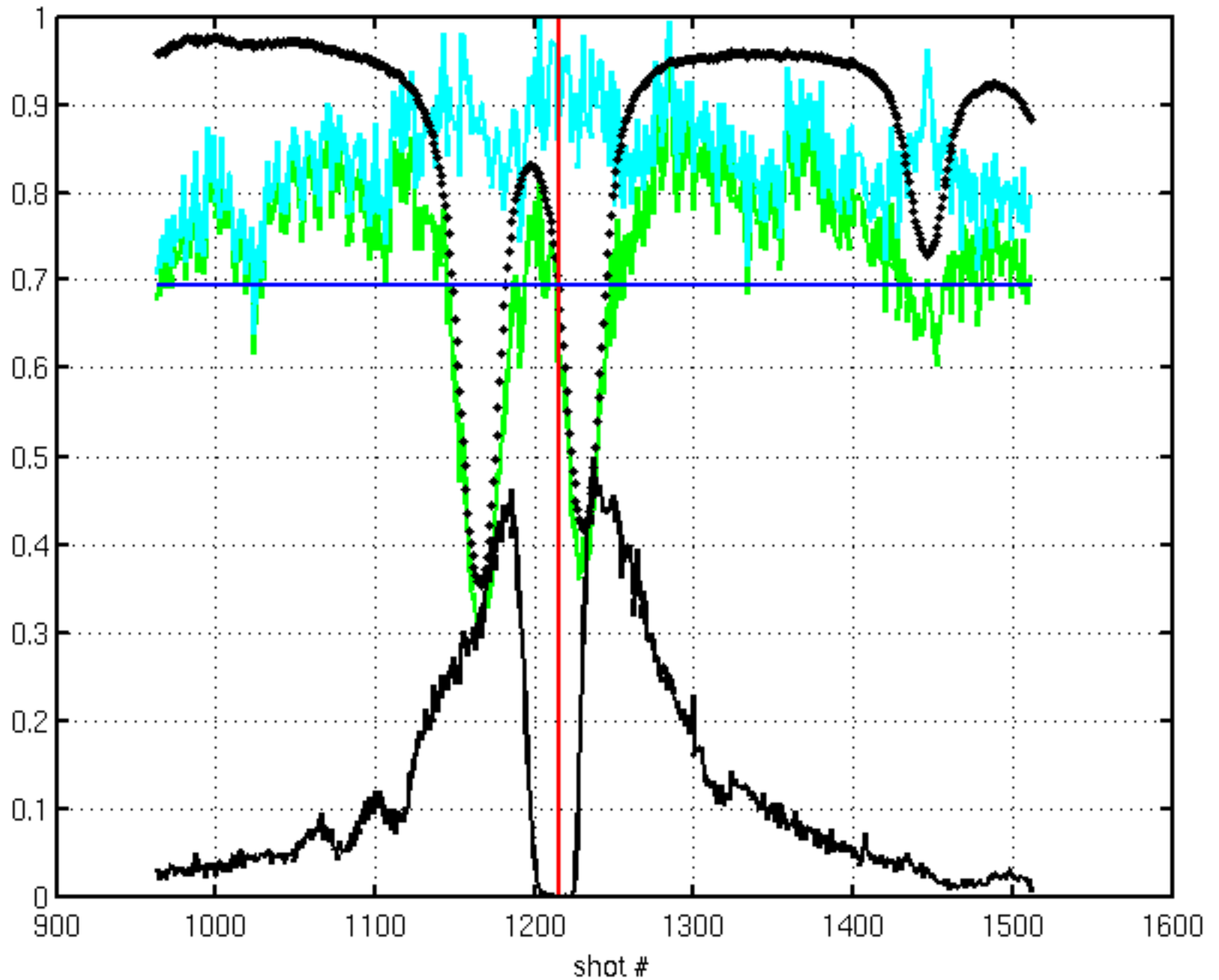


Figure 4. A block-diagram of the experimental setup.

3.2 Detector impulse response function

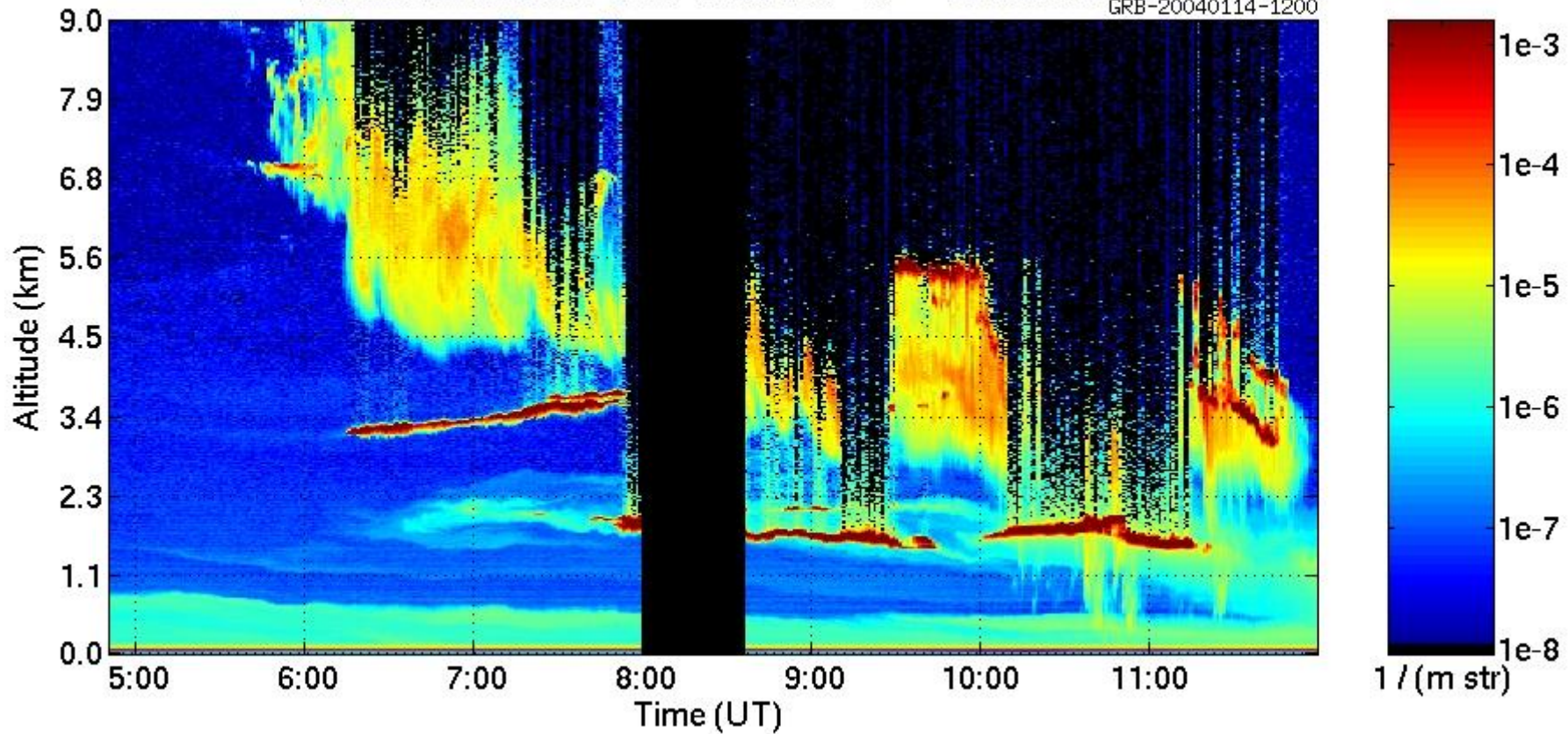
Brillouin lock parameters





Aerosol backscatter cross section $\text{m}^{-1} \text{str}^{-1}$ 14-Jan-2004

GRB-20040114-1200



Specifications

Transmitter: **GVHSRL** **Langley HSRL**

Repetition rate	4000 Hz	200 Hz
Wavelength	532 nm	532 nm
Energy	82 uJ	2.5 mJ
Ave power	339 mW	500 mW

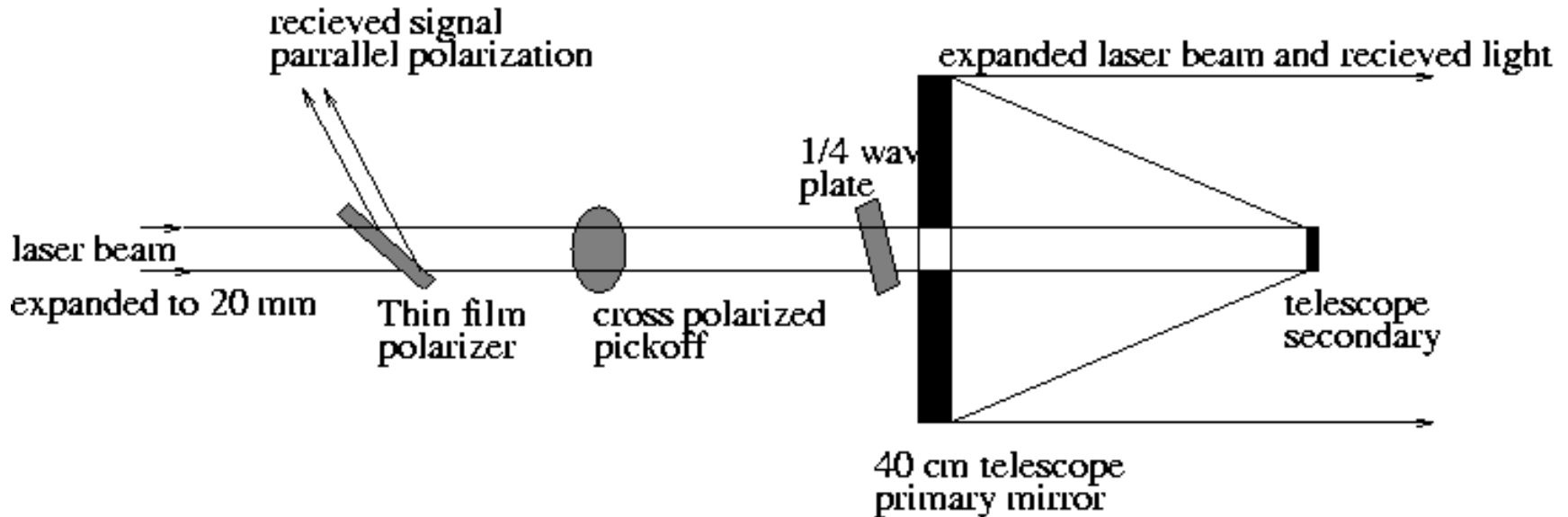
Receiver:

Aperture	40 cm	40 cm
Bandwidth	8 GHz	60 GHz
Quantum Eff	55%	10% (?)
Field of View	100 μ rad	250-1000 μ rad
Optical trans	~34%	57%

Signal strength ~ 1 0.27 (Area*Pwr*QE* η)

Sky Noise ~ 0.24 3.4 (Area*BW* Ω *QE* η)

AHSRL transmit-receive telescope



- The 20 mm diameter linearly-polarized laser beam is converted to circular polarization by $\frac{1}{4}$ wave plate before expansion 40 cm.
- The received signal is converted to linear polarization on return through the $\frac{1}{4}$ wave plate. Approx. 10% of the signal is separated to measure the cross-polarized component. The parallel-polarized component is separated from the transmit beam by the thin-film polarizer.

position: L3
PFC-107



EXIT

WICU
PFC-107

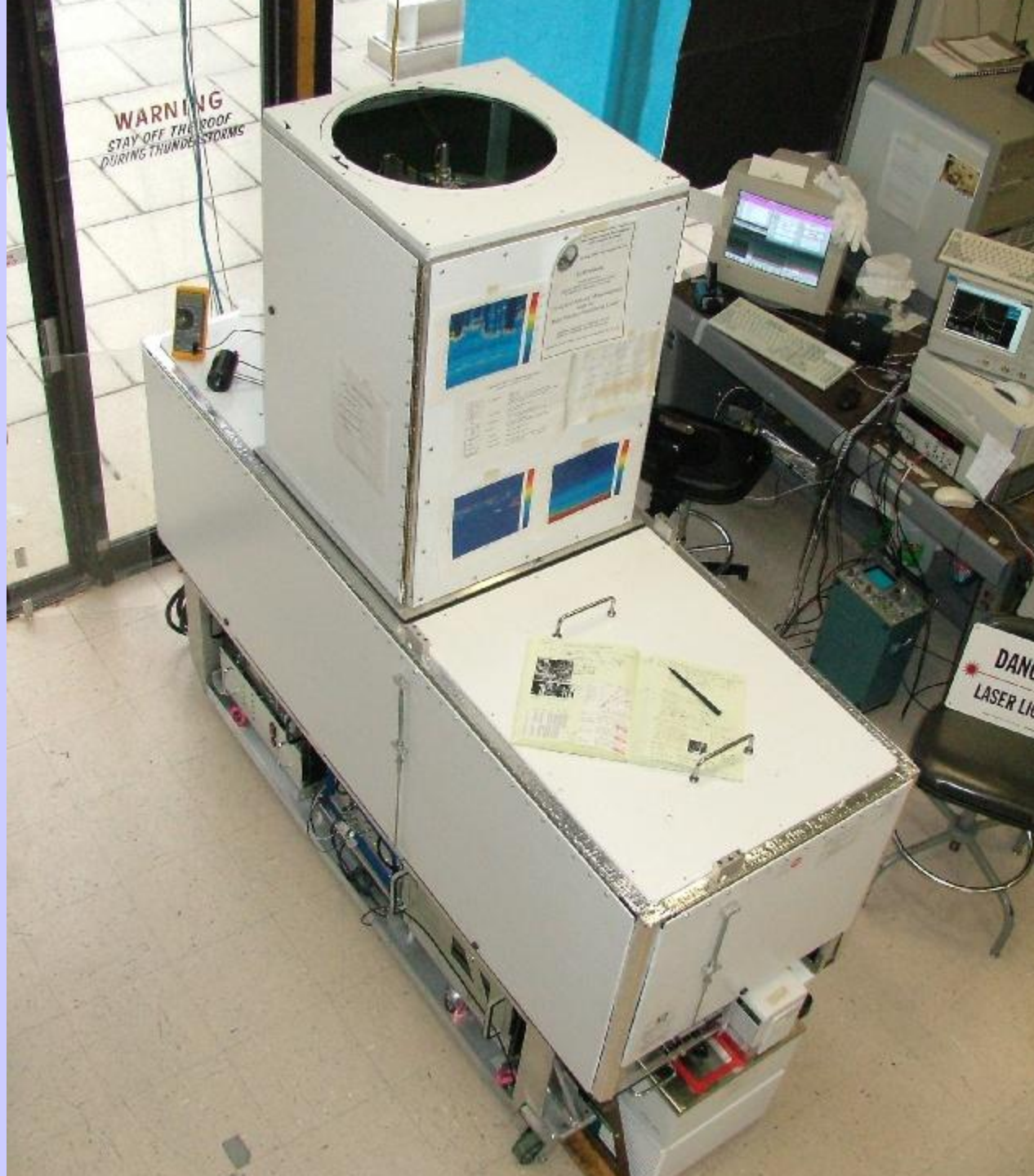
CAUTION
DO NOT TOUCH

CAUTION
PANELS ARE FRAGILE
DO NOT TOUCH PANELS

CAUTION
DO NOT TOUCH

CAUTION
DO NOT TOUCH

020



WARNING
STAY OFF THE ROOF
DURING THUNDERSTORMS

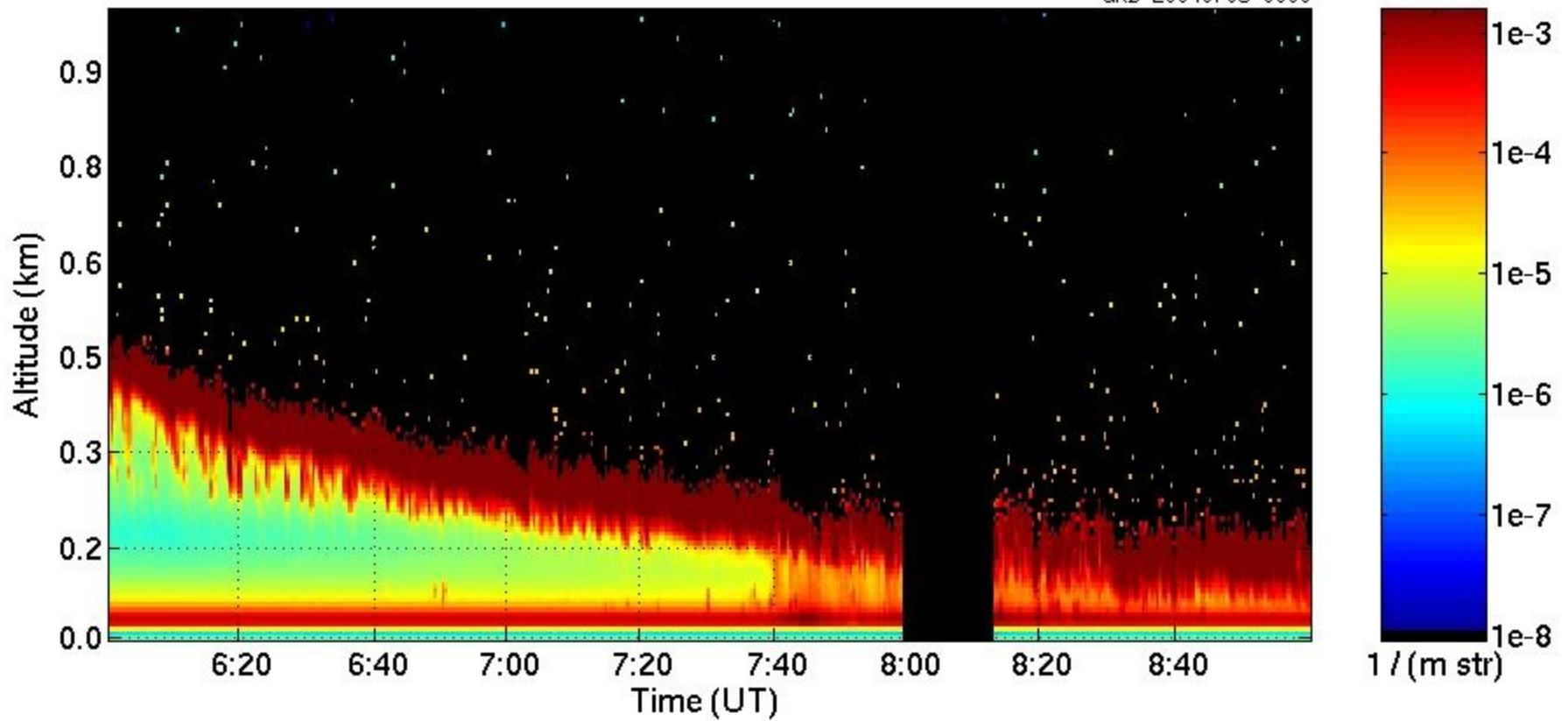
DANGER
LASER LIGHT

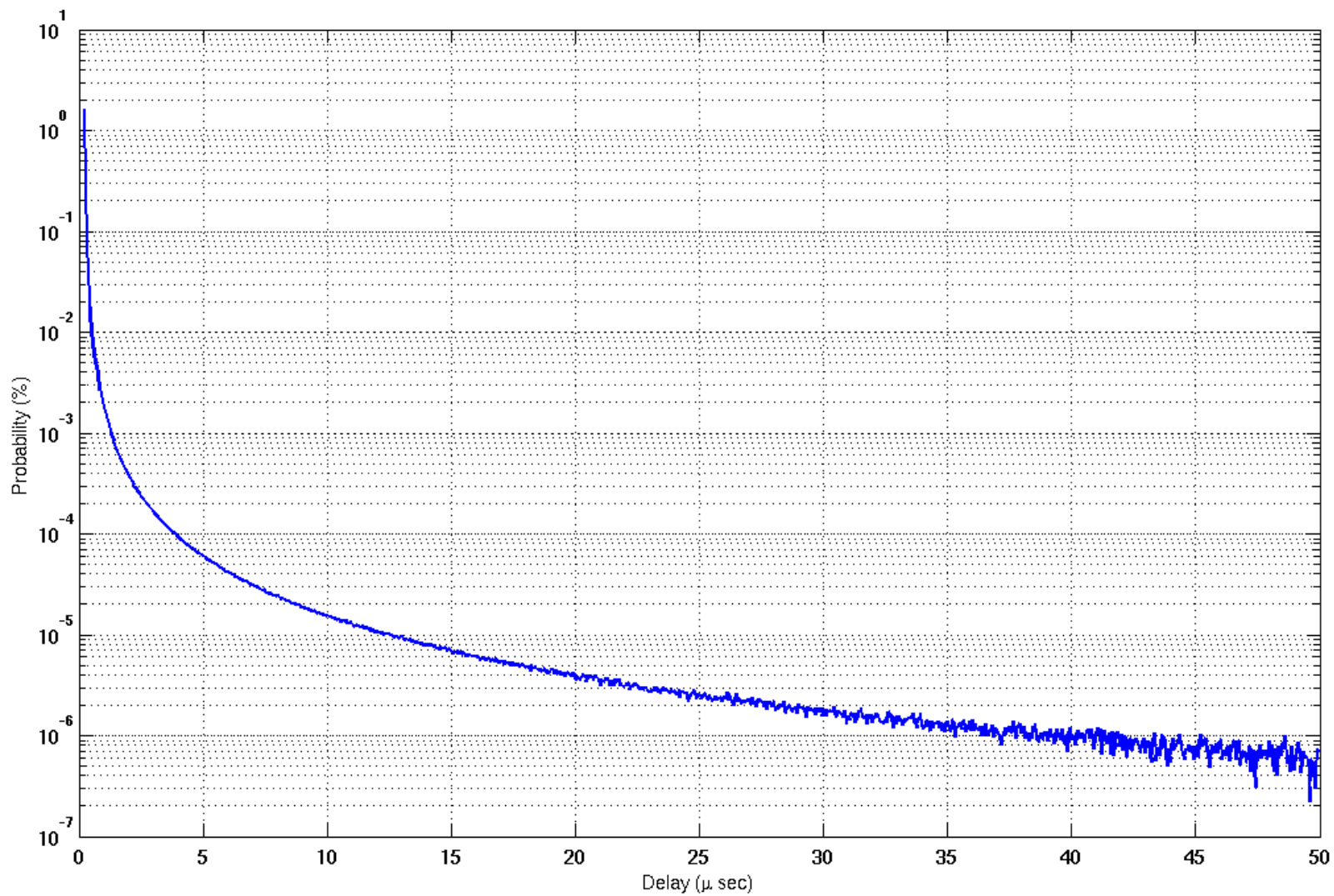
High Spectral Resolution Lidar at North Slope ARM site



Aerosol backscatter cross section $\text{m}^{-1} \text{str}^{-1}$ 06-Jul-2004

GRB-20040706-0000





Arctic HSRL Specifications

- Altitude coverage ~75m-->30 km
- Altitude resolution 7.5 m
- Time resolution :
 - -Backscatter, depolarization profiles 0.5 sec
 - -Optical depth profiles >20 sec
- Eye safe at output
- Wavelength 532 nm
- Power 200 → 600 mW
- Repetition rate 4 kHz
- Field of view 45 microradians
- Sky noise filter bandwidth 8 GHz
- Typical background noise/bin >1 photon/1000 laser pulses
- Receiver diameter 0.4 m
- I2 filter bandwidth 1.8 GHz



High Spectral Resolution Lidar
Ed Eloranta—Univ. of Wis.
<http://lidar.ssec.wisc.edu>



OD computed from average transmission 26-Sep-10 16:00 ---> 16:59

